(4)

AD-A199 402

OFFICE OF NAVAL RESEARCH

Contract N00014-87-K-0457

R&T Code 4134015———01

Technical Report No. 4

The Structure and Optical Properties of CdS
Superclusters in Zeolite Hosts

by

+Norman Herron, +Ying Wang, Mike Eddy, Galen D. Stucky, ^Dave Cox,
#Karin Moller, #Thomas Bein

submitted for publication in:
Journal of the American Chemical Society

DTIC
SELECTED
JUN 1 6 1988
H

Department of Chemistry
University of California
Santa Barbara, California 93106

May 1988

+E.I. du Pont de Nemours & Co., Central Reserach and Development Dept.,
Wilmington, DE 19898

^Department of Physics, Brookhaven National Laboratories, Upton, Long Island,
NY 11973

#Department of Chemistry, University of New Mexico, Albuquerque, NM 87131

# REPORT DOCUMENTATION PAGE

READ INSTRUCTIONS
BEFORE COMPLETING FORM

| 1. REPORT NUMBER | 2. GOVT ACCESSION NO. | 3. RECIPIENT'S CATALOG NUMBER |
|---|---|---|
| 4 | | |

**4. TITLE (and Subtitle)**

The Structure and Optical Properties of CdS Superclusters in Zeolite Hosts

**5. TYPE OF REPORT & PERIOD COVERED**

Technical

**6. PERFORMING ORG. REPORT NUMBER**

**7. AUTHOR(s)**

Norman Herron, Ying Wang, Mike Eddy, Galen D. Stucky, Dave Cox, Karin Moller, Thomas Bein

**8. CONTRACT OR GRANT NUMBER(s)**

N00014-87-K-0457

**9. PERFORMING ORGANIZATION NAME AND ADDRESS**

Department of Chemistry
University of California
Santa Barbara, CA 93106

**10. PROGRAM ELEMENT, PROJECT, TASK AREA & WORK UNIT NUMBERS**

**11. CONTROLLING OFFICE NAME AND ADDRESS**

**12. REPORT DATE**

May 1988

**13. NUMBER OF PAGES**

**14. MONITORING AGENCY NAME & ADDRESS(If different from Controlling Office)**

**15. SECURITY CLASS. (of this report)**

Unclassified

**15a. DECLASSIFICATION/ DOWNGRADING SCHEDULE**

**16. DISTRIBUTION STATEMENT (of this Report)**

**17. DISTRIBUTION STATEMENT (of the abstract entered in Block 20, if different from Report)**

**18. SUPPLEMENTARY NOTES**

Submitted for publication in Journal of the American Chemical Society

**19. KEY WORDS (Continue on reverse side if necessary and identify by block number)**

superclusters, semiconductors, zeolites, cadmium sulfide, optical properties, EXAFS, disorder

**20. ABSTRACT (Continue on reverse side if necessary and identify by block number)**

DD FORM 1473  EDITION OF 1 NOV 55 IS OBSOLETE
1 JAN 73
S/N 0102-LF-014-6601

# THE STRUCTURE AND OPTICAL PROPERTIES OF CdS SUPERCLUSTERS IN ZEOLITE HOSTS

Norman Herron and Ying Wang
Central Research and Development Department
E.I. Du Pont de Nemours & Co.
Wilmington, DE 19898
Contribution No. 4571

Mike M. Eddy and Galen D. Stucky
Department of Chemistry
University of California
Santa Barbara, CA 93106

Dave E. Cox
Department of Physics
Brookhaven National Laboratories
Upton, Long Island, NY 11973

Karin Moller and Thomas Bein
Department of Chemistry
University of New Mexico
Albuquerque, NM 87131

## ABSTRACT

Direct synthesis of CdS within the pore structure of zeolites leads to a novel supercluster with a structural geometry superimposed by the host framework. Detailed X-ray powder diffraction, EXAFS analysis and optical absorption data reveal discrete $(CdS)_4$ cubes located within the small sodalite units of the structure which begin to interconnect as the

1

88 6 14 005

loading density within the zeolite rises. The discrete cube building blocks consist of interlocking tetrahedra of Cd and S with a CdS bond length of 2.47Å. At higher loadings these cubes begin to occupy adjacent sodalite units where the Cd atoms point toward each other through the double six-rings linking the sodalite moeities with a Cd-Cd distance of ~6Å. As this three dimensional interconnection proceeds, the corresponding changes in optical properties indicate a transformation to a semiconductor supercluster with behavior intermediate between that of the discrete CdS cubes and bulk semiconductor. Semiconductor superclusters represent a novel class of materials where the 3-dimensional structure and electronic properties can be controlled by using different zeolites as the template.

The unique stability of $(CdS)_4$ clusters inside the sodalite units is due to the coordination of Cd atoms with the framework oxygen atoms of the double 6-ring windows. The stability of the supercluster comes from the interaction between $(CdS)_4$ clusters in the adjacent sodalite units. We suggest that through-bond coupling is responsible for the interaction between $(CdS)_4$ clusters.

2

# THE STRUCTURE AND OPTICAL PROPERTIES OF CdS SUPERCLUSTERS IN ZEOLITE HOSTS

Norman Herron and Ying Wang
Central Research and Development Department
E. I. Du Pont de Nemours & Co.
Wilmington, DE   19898
Contribution No. 4571

Mike M. Eddy and Galen D. Stucky
Department of Chemistry
University of California
Santa Barbara, CA   93106

Dave E. Cox
Department of Physics
Brookhaven National Laboratories
Upton, Long Island, NY   11973

Karin Moller and Thomas Bein
Department of Chemistry
University of New Mexico
Albuquerque, NM   87131

## I. INTRODUCTION:

Small metal and semiconductor clusters, having hybrid molecular and bulk properties, represent a new class of materials and are under intensive investigation. Many approaches exist for preparing these small clusters. Well-defined, mass-selected clusters up to hundreds of atoms can be generated in the gas phase using supersonic jet expansion techniques[1-3]. Many interesting properties of these "bare" clusters, including chemical reactivities, have been studied; although direct

structure determination of these clusters is still not available. Clusters

can also be prepared in the condensed phase where the environment

necessarily plays an important role. Small semiconductor clusters and

particles have been prepared in solutions[4-12], glasses[13,14], and

polymers[15,16]. In these systems, the sizes of the clusters are not as

well-defined. However, it can be varied to cover almost the entire range

from molecular to bulk[16]. Another approach, perhaps the most desirable

one, if it is generally feasible, is through systematic chemical synthetic

techniques. The synthesis of large gold and silver clusters have been

reported recently[17]. To the best of our knowledge, this has not been done

for semiconductor clusters.

Well-defined clusters can also be synthesized inside zeolites.

Zeolites are crystalline Al-O-Si materials containing pores of molecular

dimensions, interconnected by smaller windows (Figure 1). For example,

zeolite Y contains both 5Å (sodalite cage) and 13Å (supercage) pores.

Using zeolites as hosts, in principle, one can generate well-defined

clusters inside these pores. This approach has been used for generating

silver clusters inside zeolites[18]. Furthermore, by filling up all the

internal pores of zeolites, one can build novel 3-dimensional supercluster

structures that consist of individual clusters interconnected through the

windows of the pores. Using different zeolites as the template,

superclusters with different structures and electronic properties can be

built. In this paper we present the synthesis and structure determination

of CdS superclusters inside zeolites, and discuss their optical and

electronic properties. Part of the results has been presented in a previous

4

communication[19]. In a separate paper[20], we discussed the properties of selenium clusters in zeolites.

## II. EXPERIMENTAL:

### A. Synthesis of CdS/Zeolite composites

All three zeolite entrapped semiconductor materials were prepared by essentially the same procedure, illustrated here for zeolite Y. Starting zeolite materials were commercially available from Linde as zeolite 5A, zeolite 13X and zeolite LZY-52 (NaY) and were used without further purification. Hydrogen sulfide gas was from Matheson while cadmium nitrate was from Alfa and again these were used without further purification.

10g of zeolite NaY was slurried in 1000 mL distilled water and the pH was adjusted to 5 with nitric acid. 10g cadmium nitrate was added and the mixture stirred at room temperature overnight. The Cd ion-exchanged zeolite was collected by filtration and washed extensively with distilled water then suction dried to a damp powder. The material was then dried and calcined in a 12" tube furnace in flowing oxygen (100mL/min) with the powder being a maximum of 1/4" deep throughout the bed. A slow temperature ramp from room to 400°C over 2 hours followed by a hold at 400°C for a further hour gave a dry white powder. The sample was cooled in vacuo to 100°C over 1 hour and then exposed to flowing hydrogen sulfide (40mL/min) at 100°C for 30 mins - the effluent $H_2S$ being passed through hypochlorite scrubbers before being vented through an efficient fume hood. Finally the still white zeolite was evacuated at 100°C for 30 minutes in vacuum before the sample was sealed and transferred to a dry nitrogen

5

glove box for storage. During the final evacuation the white zeolite becomes pale yellow/cream and this color change is reversible in that treatment with additional $H_2S$ returns the zeolite to the original white color[21].

Variations on this basic procedure were in adjusting the original pH of the zeolite slurry to 6.5 rather than 5 for the more acid sensitive zeolites A and X. Different Cd loadings were achieved by controlling the amount of Cd in the ion-exchange solutions.

All samples were water sensitive (including atmospheric moisture) to a varying extent. Zeolites X and Y immediately become deep yellow orange upon immersion in water or any polar, non-basic solvent. Zeolite A slowly evolved a yellow-orange color over a longer (~1 hour) period when immersed in water. To avoid this semiconductor migration and aggregation the samples must be stored and handled in a rigorously dry atmosphere.

### B. Characterization of CdS/Zeolite Composites.

Chemical analyses of zeolite composites were performed by Galbraith Labs., Knoxville TN using atomic absorption. Chemical analyses of samples used in this study are listed in Table I. X-ray photoelectron spectroscopy of the samples as prepared was unable to detect any Cd in the outer 50Å of the zeolite particles even in the very highest loaded samples. This confirms that essentially all of the CdS is within the zeolite pore structure in the absence of solvent induced migration. ESR spectra of the samples showed no signal other than that expected for Fe and Mn impurities in the zeolite host. IR spectra of these materials were

unable to detect any SH groups after the final evacuation but showed the expected OH groups. Significant shifts in the framework Tetrahedral atoms (i.e. Si or Al)-Oxygen bonds (T-O bonds), as shown in Figure 2 and listed in Table II, indicate a strong interaction between the encapsulated CdS clusters and the zeolite framework which is confirmed by the x-ray results listed below.

### C. Diffuse reflectance measurements:

The absolute absorption coefficients of these semiconductor clusters were obtained using the diffuse reflectance theory of Kubelka-Munk (K-M)[22].

$$\alpha = S \cdot F(R)/2\upsilon_p \qquad (1)$$

where $\alpha$ is the absorption coefficient (in units of 1/cm, normalized to the volume fraction of the semiconductor), S is the scattering coefficient, $\upsilon_p$ is the volume fraction of the semiconductor, and F(R) is the K-M function defined as

$$F(R) = 1 - R^2/2R \qquad (2)$$

where R is the experimentally measured diffuse reflectance. The K-M function of the semiconductor, corrected for the zeolite absorption, is:

$$F(R_s) = F(R_{composite}) - (\upsilon_d - \upsilon_p/\upsilon_d)F(R_{zeolite}) \qquad (3)$$

where $\upsilon_d$ is the volume fraction of the diluent. The reflectance of the CdS/zeolite sample is measured directly if the CdS loading is low. For high-loading samples, it is necessary to dilute with either pure zeolite or $BaSO_4$ due to the strong absorption.

We have used either a Cary 14 or a IBM uv-vis spectrometer, both equipped with a dual-channel diffuse reflectance attachment, to measure the diffuse reflectance. The different responses from the two channels are corrected by taking the ratio of the diffuse reflectances of $BaSO_4$ at both the sample and reference ports. The relative reflectances of pure zeolites and CdS/zeolite composites are then measured against the $BaSO_4$ reference. The K-M function of the semiconductor, $F(R_s)$, is then calculated using equations (2) and (3), using the literature value for the absolute reflectance of $BaSO_4$[23].

To obtain the absolute absorption coefficient, one has to know the scattering coefficient of the sample. When $BaSO_4$ is used as diluent, the literature value of the scattering coefficient of $BaSO_4$ is used[24]. When the diluent is zeolite, its scattering coefficient has to be independently measured, using[22,24]:

$$S = (1/d)(R\infty/(1-R\infty)^2) \cdot \ln \frac{(R\infty R-1)(Rg-R\infty)}{(R\infty Rg-1)(R-R\infty)} \qquad (4)$$

8

where R∝, R, and Rg represent diffuse reflectances from a thick sample, a thin sample with thickness d, and the dark background, respectively. Details of this method can be found elsewhere in reference 22. Figure 3 shows the scattering coefficients of zeolite Y and mordenite that we have measured. It can be seen that the wavelength dependence of the scattering coefficient of zeolite is gradual in the wavelength region of interest. The K-M function therefore is a good representation of the absorption spectrum. In this work, we have determined the absolute absorption coefficients for certain selected samples only. The K-M function, which has the same shape as the absorption spectrum, is reported for the rest of the samples.

### D. Powder Synchrotron X-ray Diffraction.

High resolution x-ray powder diffraction data were collected for two different samples of CdS in zeolite Y on the powder diffractometer at beam line X13A at the Brookhaven National Synchrotron Light source. The samples contained 13.5Cd with 10.3S and 18.6Cd with 6.7S per unit cell (8 supercages/ 8 sodalite units). A perfect Ge(111) crystal scattering in the horizontal plane was used as a monochromator of the incident x-rays. The sample and LiF(400) analyzer crystal scatter vertically. For a full description of the diffractometer geometry at X13A see reference 25. The samples were packed into flat aluminum holders and the contents protected from moisture by sealing with thin beryllium foil. The data were collected by step-scanning from 5° to a maximum of 98° in intervals of 0.01° for periods of 2 to 10 seconds. Longer counting times are required at higher scattering angles to counteract the fall off in the form factor. The

9

wavelength was determined to be 1.5466Å by calibration with a Si standard. The sample container was rocked 2° at each data point to reduce the effects of preferred orientation. An ion-chamber filled with nitrogen was placed before the sample in order to monitor the incident beam intensity. Beam size was 2.5x1mm in the horizontal and vertical directions respectively and the intensity at the sample position was ~10e$^{10}$ photons/sec for a storage ring current of 100mA

The Be foil protected the samples from moisture successfully as judged by the sample coloration after data collection. Since Be is highly crystalline, the foil showed only a small number of sharp reflections which could be easily excluded from the refinement with a minimum loss of zeolite data.

The structural refinements were carried out using standard profile refinement techniques. The initial normalizations of the data were performed using programs available at Brookhaven while for structural refinement a modification of the original Rietveld program was employed. This program incorporates the Voigt peak shape description that is essential for analysis of powder patterns collected using the two crystal configuration employed at X13A. The extra-framework material was revealed by standard Fourier methods.

### E. Extended X-Ray Absorption Fine Structure Studies

EXAFS experiments were carried out at the X-11A beamline at the Brookhaven National Synchroton Lightsource with a stored electron energy of 2.5GeV and ring currents between 40-130 mA. Transmission Cd K-edge (26,711 eV) data were collected using a Si(400) crystal monochromator

and ionization chambers filled with Ar($I_0$) and Kr(!).

The zeolite samples were embedded in a 1:1 dodecane/octadecane mixture under inert atomsophere in a Vacuum Atmospheres drybox. They were kept under nitrogen until the EXAFS measurements were carried out. Data collection was done at liquid nitrogen temperature, scanning up to 1500 eV above the absorption edge. At least two scans per sample (20 min.) were taken.

The sample thickness was calculated to give an absorption step $\mu x$ between 0.7-1 and a total absorption of less than 2. The data were analyzed with the University of Washington EXAFS program following published procedures [26]. Background removal was accomplished using a cubic spline function. The resulting EXAFS modulations were weighed by $k^3$ (k, electron wavevector) and Fourier transformed (FT) over a range k = 2-15 ($\text{Å}^{-1}$). Data of reference and unknown were consistently treated as similarly as possible to avoid artefacts.

EXAFS measurements were performed on the following samples:

CD1    $Cd_{18.3}Na_{19.4}Al_{56}Si_{136}$

CD2    $Cd_{5.8}S_{5.0}Na_{44.4}Al_{56}Si_{136}$

CD3    $Cd_{15.3}S_{6.1}Na_{26}Al_{56}Si_{136}$

CD4    $Cd_{18.6}S_{6.7}Na_{19.4}Al_{56}Si_{136}$

References used were: CdS, $Cd(NO_3)_2 \cdot 4H_2O$, and PdO. EXAFS reference parameters were extracted as follows:

PdO was used a) as reference for the Cd-oxygen coordination sphere by applying an inverse Fourier transformation (IFT) to the first shell

(Refernce values R = 2.01Å, N = 4 [27]), and b) as reference for the Cd-Cd contribution in CdO cluster (IFT on the 3. shell, ref. values R = 3.42, N = 8). Phase- and amplitude transferability can be assumed, since Pd and Cd are close in the periodic table. Occurrence of four, large deviating bond distances of cadmium nitrate (2.26-2.59 [28]) made this sample only useful as a qualitative reference for the Cd-O scatter pair.

CdS supplied reference data for a) the sulfur scatterer (Reference values R = 2.52Å, N = 4 [29]) and b) for the Si/Al neighbor contribution from the zeolite framework. The same argument as above holds for using CdS as reference for Cd-Si/Al. Distinction between Si and S in the unknown sample by using the same reference is easily obtained, because their possible bond distance are about 1Å different (Cd-S 2.5Å, Cd-O-Si 3.2-3.5Å). Application of CdS for a 2. shell Si reference is assumed to introduce only minor errors, since bond angles between Cd-O-Si are <150° and will therefore not contribute to multiple scattering. A mean free path correction was applied in all instances where the bond distance of the reference and the actual value differ by more than 0.1Å (see Table III).

## III. RESULTS:

### A. Optical properties of CdS clusters in zeolite Y.

The optical absorption spectra of CdS in zeolite Y are shown in Figure 4 and 5. Depending on the concentration of CdS, the optical spectra can be distinctively different. Below 4±1 wt% of CdS loading, the absorption spectrum has a shoulder near 280-290 nm. Above 4±1 wt% of CdS loading, the spectrum shifts to the red and shows a shoulder near 350-360 nm (Figure 4). Once above this critical threshold concentration

(4±1 wt%), no major change in the absorption spectrum can be observed (Figure 5).

As shown in Figure 4, both the low-loading and high-loading CdS/zeolite Y spectra are blue-shifted from the bulk CdS spectrum. If CdS is removed from the zeolite pores by exposing the sample to moisture, the absorption spectrum then evolves into the bulk spectrum[19]. This deviation from the bulk spectrum as the semiconductor particle size decreases, is now commonly observed among colloidal semiconductor particles and often referred to as the quantum size effect[4-16]. The origin of the quantum size effect is simply due to the discrete nature of the conduction and valence band and can be qualitatively understood on the simple Huckel MO level[16,19].

The unique concentration dependence of the absorption spectra of CdS in zeolite suggests a percolative phenomenon[30]. At low concentrations, CdS exists as isolated molecules or small clusters within the pores of zeolites. At high concentrations, they aggregate together, through the windows of the pores, to form a supercluster by a percolative process. The percolation threshold is around 4±1 wt%. In the next section we will present results from a x-ray diffraction study and will show that these conclusions are supported by the structural data and consistent with the percolation theory.

The concentration dependence of the emission spectra also parallels that of the absorption spectra. At low CdS concentrations, no emission can be seen down to 4 K (except the weak zeolite emission). Once above the threshold concentration of 4±1 wt%, emissions due to defects of CdS can be observed (Figure 6). The excitation spectrum shows a pronounced

13

peak at 350-360 nm, consistent with the shoulder of the absorption spectrum of CdS/zeolite. Details of the photophysical study will be published in a separate paper.

### B. Structure of CdS clusters in zeolite Y.

The observed, calculated and difference profiles for the two zeolite Y samples of different CdS loading are illustrated in Figure 7. The refined atomic and profile parameters are given in Table IV with selected bond lengths and angles in Table V. Excellent refinements were obtained for both the zeolite samples and are reflected in the small values of $\chi^2$.

The refined structures for both samples show a zeolite framework which is very similar to that of the parent sodium zeolite. The average T-O bond length (Table IV) is in excellent agreement with that expected for a zeolite of this Si/Al ratio (2.61). Space group Fd3m (origin at center) was used throughout the refinements which assumes a random arrangement of silicon and aluminum in the tetrahedral atom positions and a suitable scattering length was calculated based on the analyzed Si/Al ratio. This proved adequate for refinement purposes. The powder peak shapes could be accurately described by the convolution of Gaussian and Lorentz functions - the Voigt function. No asymmetry could be detected in the low angle reflections indicating that the analyzing crystals work well at removing sample displacement effects. The variation in the refined values for U,V,W (the Gaussian component) from sample to sample arise from the differing amounts of disorder present in the zeolite Y cages.

While the overall framework structure is as expected there are small variations in the individual T-O bond lengths. These are rationalized

14

in terms of approach of both sodium and cadmium cations and both samples show these variations. The lower loading sample (Cd13.5) has most of the sodium cations located at the SII site illustrated in Figure 8a. SII is within the 13Å supercage of Y and results in trigonal coordination for the Na. This location has been shown to be the most energetically favorable site for sodium[31]. The $Cd^{++}$ ion is located primarily at the SI' site illustrated in Figure 8b. This site, inside the sodalite units of the framework, is preferred by multivalent cations because some of the high charge density can be compensated by hydroxyl anions at the SII' site also in the sodalite cage (Figure 8c). The Cd at SI' has an octahedral coordination geometry resulting from trigonal coordination to framework oxygens of the sodalite six oxygen ring (which is part of the double six-ring interconnects of the Y structure) Cd-O 2.48Å and the three SII' atoms Cd-S 2.45Å or Cd-O 2.28Å. The two alternative SII' sites were detected in difference Fourier syntheses and refined separately as S or O (from water or hydroxyl). The overall structure of the sodalite cage entrapped species is therefore a distorted cube of $Cd_4S(O)_4$ as depicted in Figure 9. Remaining electron density assigned to Cd is located in the 12-ring window site III (Figure 8d) and is bound to two framework oxygens at 2.57Å and 2.72Å and two water molecules at 2.66Å and 2.50Å. The total Cd content based on occupancy of these two positions is 11.8 in reasonably good agreement with that found in chemical analysis (13.5).

In the higher Cd loading sample the exact same structure is maintained but now the occupancy of the SI' site has increased so that 37% of these sites are now filled. Bond lengths within the cube and to the framework oxygen atoms remain unchanged.

In both cases we find no evidence for sulfur outside the sodalite cages so that all CdS species must reside there. The high occupancy of the sulfur sites within the sodalite cages is a little puzzling since the chemical analyses have shown considerably lower S contents. This may be explained either by a mixed occupancy of the SII' site by both sulfur and oxygen (from water or hydroxyl) so boosting the apparent occupancy by S or else a problem with the chemical analyses of S in these materials. This latter is a distinct possibility in view of the equilibrium between CdS and $H_2S$ discussed in section IV.F below. It is conceivable that the freshly prepared samples used in the x-ray work were slowly evolving $H_2S$ continuously prior to their chemical analysis resulting in the S content discrepancies.

### C. EXAFS Analysis

The experimentally observed EXAFS modulations contain information about the local environment of the intrazeolite Cd(II) ions which is complementary to our X-ray powder diffraction results above. Each spectrum is a superposition of contributions of different coordination shells around the Cd absorber atom. After subtraction of the background, normalization and Fourier transformation, a separation of different shells on the radial coordinate (R-space) is obtained. All peaks are shifted to lower R values due to phase shift effects. Figure 10 shows FT's of sample CD1, CD2 and CD3. Sample CD4 is very similar to CD3 and is not further investigated.

We discuss first the data analysis of the Cd-exchanged and oxygen-treated sample CD1, which is a precursor for the $H_2S$-treated zeolites. As indicated by multiple nodes in the CHI functions, these EXAFS data represent a convolution of several closely positioned backscatterer contributions. In a first approach to obtain information about coordination distances (R) and numbers (N), each of the two broad peaks in the FT was backtransformed and fitted separately with appropriate references. An attempt to fit the first peak (IFT: 1.3-2.3Å) with only one oxygen distance failed. Best fitting results were obtained using three different Cd-O bond lengths, the result of which is shown in Figure 11a. A qualitative comparison of the original first shell CHI function with that of cadmium nitrate supports the presence of several Cd-O distances: The $Cd-O_8$ sphere in $Cd(NO_3)_2 \cdot 4H_2O$ is composed of 4 Cd-O distances ranging from 2.26 to 2.59Å, and its CHI function is almost identical with that of sample CD1.

A similar technique was applied to the second shell of CD1 (IFT 2.3-3.8Å). PdO and CdS were used both isolated and combined as references for Cd-Cd and Cd-Si scatter pairs (see experimental). The best fit is shown in Figure 11b. The resulting values for bond distances, coordination numbers and Debye-Waller factors of both shells were finally used for a fit of the whole data file (IFT: 1.3-3.8Å) and were refined to the values listed in Table III. The final fit of the CHI function and its Fourier transformation into R-space is shown in Figure 12.

The results as shown in Table III are interpreted in terms of a distorted cadmium oxide cube located in the sodalite cavities of the zeolite framework.

17

1.     From the combined presence of oxygen in the first shell and Si/Al neighbors in the second shell it is clear that the $Cd^{2+}$ ions are located in zeolite extra-framework cation positions.  A Cd-O distance of 2.44Å is common for cations stablized in the $C_{3y}$ six-ring coordination sites of faujasites.  A similar value (2.48Å) was also extracted from X-ray diffraction data in this work and attributed to Cd in SI' positions (Figure 8b).  In agreement with the X-ray data, we can exclude the occupation of the SI sites by Cd(II) in double sixring positions.  The EXAFS data could not be fitted with the expected longer coordination distances of 2.6Å.

2.     Additional oxygen neighbors (SI' requires only 3 per $Cd^{2+}$) detected at relatively short distances of 2.25 and 2.34Å are assigned to Cd-OH- or $Cd-H_2O$ neighbors in a $Cd_4O_4$ cube in the sadalite cage, which formally would result in three more O atoms per $Cd^{2+}$.

3.     A signficant fraction of the second shell is due to Cd-Cd scattering at R = 3.29Å.  A fit with a similar quality was also obtained with the second shell solely composed of Si/Al neighbors.  The total number of Cd-(Si/Al) would then be higher than 12 (uncorrected).  We can exclude this alternative because it would require that all Cd would reside in SI positions.  A further indication for the presence of cadmium neighbors in the second shell is a positive peaking of the imaginary part in that shell if a phase correction for cadmium is applied.

A similar model based on a $Cd_4(O_w)_4$ cube was proposed by Calligaris et. al [32], who found $Cd^{2+}$ in SI' positions and $H_2O$ occupying SII' sites in a partially dehydrated CdY-zeolite.  The Cd bond distances to zeolite oxygen (2.40Å) and to oxygen of zeolite water (2.36Å) closely

18

resemble our results. It appears that oxygen species at or close to SII' positions are indispensible as shields of neighboring divalent cations located in SI'. A similar stabilizing effect of OH⁻ has been proposed in an X-ray-diffraction study of Ca faujasites. The data were consistent with a $Ca^+(OH)_2Ca^+$ double hydroxide bridge arrangement (Ca in SI', OH in SII') which represents a fragment of the $Cd_4O_4$ cube proposed in the present study [33]. It should be noted that our results for Cd-O and Cd-Cd distances are very close to those of cubic CdO (NaCl type) (Cd-O, 2.35 and Cd-Cd, 3.32Å, [34]). The intrazeolite $Cd_4O_4$ cube may therefore be considered as a small fraction of CdO. Deviations in N found between the proposed cube model and the listed results are within the limits of the fit.

Treatment of the cadmium exchanged samples with $H_2S$ at 100°C causes only moderate changes in the overall appearance in the EXAFS spectrum (compare Figure 1a and 1b). Use of a difference-file technique allows us to detect and analyze the new Cd-S backscattering contribution: Subtracting the datafile CD1 from CD2 results in a spectrum with a major peak resembling position and imaginary part of bulk Cd-S (see Figure 13a; only the magnitude is shown for clarity). This difference file was fitted with CdS. The best fit results were used to calculate a Cd-S contribution (R = 2.52Å, N = 1.5, $\Delta SS$ = 0.0009Å2), which was subtracted from the original CD2 data file. As shown in Figure 13b, the imaginary part is now very similar to that of CD1. A fit of the entire data range resulted in values given in Table III. The reaction with $H_2S$ causes a reduction of the total number of first shell Cd-O scatterers, while the second shell values

19

of CD-(Si/Al) and Cd-Cd are unchanged. We conclude that 1) the overall structure of the Cd arrangement in the zeolite is unchanged upon reaction with $H_2S$, and 2) about half of the oxygens in the cube are replaced by sulfur. These results are consistent with the XRD data, and beyond that, they indicate the presence of small, rather localized $Cd_4(O,S)_4$ units in the zeolite rather than extended chains with lower local coordination number. It is not clear at this point if the sulfur resides in the zeolite as $H_2S$ or as $S^{2-}$ (see below).

Samples CD3 and CD4 are distinguished from CD2 by a strong decrease in the magnitude of the second shell. Consequently, the number of the Si/Al and Cd neighbors is markedly reduced. Fit results presented in Table III show only Si/Al scatterers listed however, a small amount of Cd ($N = <1$) with concomitant reduction of N for Si/Al would result in a fit of comparable quality. Bond distances of the oxygen neighbors are close to sample CD1, but the coordination numbers are considerably smaller. We suggest that in these samples the $Cd^{2+}$ ions are still located in lattice coordination sites. It seems that the cubes have been partially disrupted as indicated by the loss of strongly scattering Cd neighbors.

In conclusion, the EXAFS data show that the addition of $H_2S$ to $Cd^{2+}$- exchanged zeolites does not displace Cd from zeolite cation positions. Furthermore, the formation of bulk-like CdS can certainly be ruled out by our EXAFS studies. It is shown that sulfur is located in the neighborhood of Cd. It appears that the sulfur is incorporated into $Cd_4O_4$ cubes present in Cd exchanged and oxygen-treated samples. Since a total

removal of intrazeolite water is difficult, the absolute amount of residual water may differ in our samples. The formation of $Cd_4(O,S)_4$ cubes appears to require the presence of donor ligands, e.g., OH⁻, water or sulfur species.

## IV. DISCUSSIONS:

### A. Why $(CdS)_4$ clusters are so stable inside the sodalite cages?

The first thing to note from the x-ray diffraction study is that all the $(CdS)_4$ clusters reside in the smaller sodalite cages, not in the larger supercages. This initially surprising result can be immediately understood when one considers the stability of these cubic clusters. In a bare cubic $(CdS)_4$ cluster, every Cd atom is coordinatively unsaturated. The need to satisfy this unsaturation through rehybridization provides a tremendous driving force to break up the cube. The only way to have a stable cubic $(CdS)_4$ cluster is to passivate the cube surface with the surrounding medium, in this case, the sodalite cages. Examination of the x-ray data reveals that every Cd atom is surrounded by 3 oxygen atoms of the 6-ring windows of the sodalite cages (Figure 14). The Cd-O distance, 2.48Å, is somewhat larger than the typical Cd-O bond length of 2.348Å[35]. Four double 6-ring windows, arranged in a tetrahedral symmetry, match perfectly with four tetrahedrally arranged Cd atoms of the cube. The saturation of Cd coordination requirements by the framework oxygen atoms in the sodalite units is therefore the primary mechanism for the

stability of $(CdS)_4$ clusters. In the 13Å supercage, only one Cd atom of a cube could coordinate with the framework oxygens. This explains the instability and the absence of $(CdS)_4$ cube in the supercages. Our result also suggests that larger size CdS clusters should be stable in the supercage. At present, with the ion-exchange method the highest CdS loading which can be achieved is 23 wt% which just about fills the sodalite units. In order to fill up the supercages, different synthetic approachs are needed.

The stabilizing role of oxygen atoms in zeolites may not be unique. We note that most of the media used for preparing II-VI and IV-VI semiconductor particles, such as polymers[15,16], glasses[13-14], water and alcohols[4-12], all contain oxygen atoms. Their presence may serve a purpose, namely, to passivate the particle surface.

### B. From clusters to superclusters

The optical spectra of CdS in zeolite Y at low loading levels ($< 4\pm1$ wt%) are quite different from those at high loading levels, as shown in Figure 4. We assign the spectrum at low loading level to isolated $(CdS)_{1-4}$ clusters, and the spectrum at high loading level to aggregated clusters. Since the locations of each individual cluster within the aggregates are well-defined, with structural geometry imposed by the zeolite framework, it is appropriate to refer to these aggregates as superclusters.

The uncertainty of the cluster size at low loading levels arises from the symmetry properties of the sodalite cages. X-ray diffraction data of low-loading CdS/zeolite Y sample shows that Cd atoms are located at the

four SI' ion-exchange sites (Figure 8b). Due to the low loading level, it is possible that these SI' sites are only partially occupied by Cd. The exact location of the Cd atom among the four SI' sites cannot be determined by x-ray since they are all equivalent. Therefore we can only assign the observed spectrum to $(CdS)_{1-4}$ clusters. Because of the enhanced stability of $(CdS)_4$ inside the sodalite cage and the known instability of CdS molecules[36], we believe that $(CdS)_4$ is the more likely species present. We also note that $H_2S$-loaded zeolite has an absorption band in the 280 nm region which can interfere with the CdS cluster spectrum[37]. We have observed abnormally strong absorption in the 280 nm region when the CdS/zeolite sample has excessively large S/Cd ratio which we believe is due to the presence of $H_2S$. The spectrum reported here at low-loading level comes from a sample with an excellent 1:1 Cd/S ratio.

Once the CdS loading level exceeds the critical threshold of $4\pm1$ wt%, the absorption spectra shift to the red and become independent of the CdS concentration, up to the highest loading level that can be achieved by the ion-exchange method. The absorption spectrum contains a shoulder near 350-360 nm, most likely due to the exciton transition. Colloidal CdS particles with sizes of 25-30 Å show a similar absorption spectrum[6c]. This implies that the size of the supercluster must be in a similar size range. Interestingly, the critical threshold concentration of $4\pm1$ wt% corresponds to the concentration at which, statistically, CdS clusters must now populate adjacent sodalite units. The rather abrupt transition further suggests that the cluster aggregation process may be percolative.

For a 3-dimensional percolation process, the percolation threshold is predicted to be around 15 vol%[30]. If we consider the total free volume of zeolite Y (0.48 mL per 1 mL of zeolite), then 4 wt% CdS corresponds to only 2.3% by volume based on bulk density of CdS (4.82 gm/mL). However, x-ray study shows that all of the CdS clusters reside in the sodalite units and become unstable in the supercages, which suggests that only the free volume of the sodalite cages should be considered (0.08 mL per 1 mL of zeolite). In this case, 4 wt % CdS corresponds to 14 vol %, in excellent agreement with the percolation theory.

A coherent picture emerges from the x-ray and optical data in which isolated $(CdS)_{1-4}$ clusters exist at low-loading levels but percolate to form large superclusters at high-loading levels. It is important to realize that in a supercluster each individual $(CdS)_4$ cluster interacts with the others electronically through the sodalite cage windows (we will discuss the interaction mechanism in the next section). This is analogous to the much studied superlattice structure in solid state physics[38] where thin layers of semiconductor are separated by, and interact through, thin layers of a different semiconductor. Semiconductor-loaded zeolites therefore represent a three-dimensional analog of the superlattice structure where the spatial arrangement of the semiconductor clusters is controlled by the zeolite host framework structure. By using different zeolites as the template, superclusters (or superlattice) with different three-dimensional structures and electronic properties can be designed and built. We believe this truly represents a novel class of materials.

24

We also note that if one can simply fill up all the supercages in zeolite Y, then a different supercluster is generated which has different structure and optical properties from the ones reported here. We estimate this should occur at about 35 wt% CdS loading level which, unfortunately, cannot be achieved with the currently used ion-exchange method.

### C. Possible interaction mechanism within superclusters.

We now discuss the possible interaction mechanism between cubic $(CdS)_4$ clusters within a supercluster. In zeolite Y, two $(CdS)_4$ clusters are separated by a double six-ring window (3Å width) of the sodalite unit (Figure 15). The two cubes face each other through the Cd atoms at the vertices, the Cd to Cd distance being ~6Å. This is too long a distance for direct interaction through space (i.e. too long for direct overlap of the wavefunctions). The only other alternatives for such a long range interaction are: (1) through the zeolite framework, or (2) through bonding with species trapped inside the double 6 ring window, such as Cd or S. Thorough examination of the x-ray data shows that the electron density inside the double six-ring window is very low. This eliminates the possibility that either Cd or S is trapped inside the window. Interaction through the zeolite framework thus remains to be the most likely mechansim.

Through bond interaction is a well-established concept used to describe long range interaction between orbitals that are connected by sigma bonds[39,40]. Most of the studies involve C-C sigma bonds as the intervening orbitals. It has been shown that (1) through-bond interaction can extend over very long distance; up to 6 sigma bonds has been

25

demonstrated[40]; and (2) through bond interaction is sensitive to the conformation of the molecule. For example, in dehydropolyenyl, strong through-bond coupling exists only when the radical lobes and the carbon chain are in trans-conformation; cis-conformation gives weak interaction[39].

To apply the through-bond interaction concept to CdS in zeolite, we view the 6-member ring windows of the sodalite units as the intervening bridges. Adjacent $(CdS)_4$ clusters interact through these Cd-O-Al-O-Si-O-Cd bridges, which contains 6 sigma bonds. Such interaction is possible because of the strong coupling between Cd and O atoms as revealed by x-ray and pointed out in section A. For zeolite Y there are a total of 6 such bridges for interaction. The existence of 6 bridges should be especially effective in promoting the through-bond interaction since the interacting orbitals can have greater flexibility in choosing the bridge with the right conformation for interaction. The effectiveness of O-Al-O-Si-O bridge compared to the commonly studied C-C bridge is unknown. A recent study[41] shows that an Si-Si bond is more effective than C-C bond in promoting the through-bond interaction.

It is also interesting to note that not only the adjacent $(CdS)_4$ cubes can interact through the O-Al-O-Si-O bridges, but Cd atoms in the same cube can also interact with each other through the same bridge. We believe this through-bond interaction *between* and *within* the $(CdS)_4$ cubes provides the "glue" for stabilizing the CdS supercluster. If we take 290 nm as the absorption edge of isolated cluster and 350 nm as that of the supercluster, then the strength of the through-bond interaction is

estimated to be about 0.7 ev, which is consistent with the known values of through-bond interaction[39,40].

The x-ray and optical data presented above indicate that CdS clusters can interact through the zeolite framework to form an extended supercluster structure. This suggests that different types of superclusters can be built with the same $(CdS)_4$ building block by using different zeolites as the templates. An ideal candidate to demonstrate this principle is zeolite A, which is distinctly different in construction from Y in that here the sodalite units are linked together via double four rings in a cubic array (Figure 16). In zeolite A, the $(CdS)_4$ clusters in the neighboring sodalite units are expected to face each other through the facets of the cube separated by ~9Å (Figure 1b), instead of the vertices as in zeolite Y (Figure 15). Preliminary results show the exciton shoulder of a CdS supercluster in zeolite A is now located near 320 nm, instead of 350 nm observed for CdS in zeolite Y. If the structure of CdS clusters in zeolite A is the same as in Y (we have no reason to believe otherwise), then the data shows a very interesting orientational effect on the optical properties of CdS superclusters. Further studies, including structure determination using synchrotron x-ray diffraction, are in progress and will be published when completed.

### D. Spectral broading mechanisms

It is important to realize that although the size of the CdS cluster in zeolite is well-defined, i.e. a $(CdS)_4$ cube, the size of the supercluster is not. In an ideal situation, if one fills up all the sodalite cages with CdS,

then the size of the supercluster is equivalent to the size of the bulk zeolite crystals. In reality, the ion-exchange method cannot totally fill up the sodalite cages. In addition, a high density of defects (usually extra Cd) and disorder exist with the current preparation procedures. These partial vacancies and imperfections break up the supercluster and introduce inhomogenity in the supercluster size distribution, which is the primary reason for the broad exciton absorption peak that we observed. From the low temperature excitation spectrum of CdS supercluster in zeolite 13X (Figure 6), the exciton width is about 3000 cm$^{-1}$ at 4 K. This is much broader than one would expect from a perfect supercluster.

Broadening due to size distribution of supercluster can eventually be eliminated by improved synthetic procedures, as will be discussed in section F. An intrinsic mechanism that cannot be eliminated is the phonon broadening. As the semiconductor particle size decreases, the coupling of electronic transition to surface and host phonons, especially high frequency ones, becomes important. This gives rise to multiphonon sidebands and spectral broadening. We note that one of the novel features of CdS superclusters in zeolites is that every CdS in the supercluster is on the "surface". Strong coupling with the host lattice occurs through the interaction between Cd and framework oxygen. One would therefore expect the phonon coupling mechanism to become very effective. In a subsequent paper on the photophysical properties of CdS superclusters, we will present experimental data to demonstrate these points.

## E. Effects of the environment.

It is clear from the above discussion that interaction with framework oxygen is necessary to stabilize the $(CdS)_4$ clusters. It is then interesting to ask what effect this interaction has on the optical properties of $(CdS)_4$ clusters. In principle, the optical properties of very small semiconductor particles can be modified through interacting with the surrounding environment, the extent of the modification depends on the strength of the interaction. In the extreme case of very strong interaction, the semiconductor itself can be destroyed[21]. For example, we have shown that CdS is unstable in the presence of $H_2S$, which reacts with CdS to form $Cd(HS)_2$[21]. We believe that oxygen containing media such as zeolites, glasses, polymers, and alcohols have relatively weak interaction with semiconductors such as CdS and PbS, and the effects on their absorption spectra should be small. This is supported by the observation that the spectra of PbS in ethylene-15% methacrylic acid copolymer film, in zeolite Y, and in argon matrix are all very similar[16].

Although the effects of zeolite framework on the CdS absorption spectrum may be small, its effects on the the excited state relaxation processes of CdS supercluster can be very large. This is analogous to the solvent effects on the photophysics of a molecule. Often the excited state molecular relaxation processes are very sensitive to the solvent, while the absorption spectrum is only weakly perturbed by the presence of solvent. We will discuss these results in a subsequent paper on the photophysical properties of these superclusters.

### F. Synthesis of clusters and superclusters.

Finally we discuss some of the problems encountered during the synthesis of CdS superclusters in zeolites that affect the quality of the superclusters. Possible improvements are also discussed.

While the synthetic approach outlined in the experimental section is straightforward and leads to materials containing CdS as expected, the control of the Cd/S stoichiometry presents considerable challenges. If one considers the chemistry involved in the formation of the CdS clusters (eq. 5)

$$Cd^{+2}Zeol^{-2} + H_2S \; <======> \; CdS \; + \; 2H^+ + Zeol^{-2} \quad (5)$$
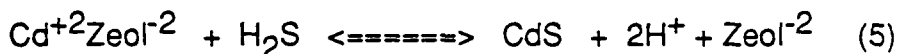
it is clear that the reaction as written is readily reversible, ie. while CdS is generated, the protons of the $H_2S$ reagent become the zeolite charge compensators forcing the CdS clusters to reside in an extremely acidic enviroment. In such an environment CdS is unstable with respect to the dissociation into Cd ions and $H_2S$. Therefore, the CdS content of the zeolite is dependent on the position of the equilibrium in eq. 5 and thus on the partial pressure of $H_2S$ present. We find that, as a result, it is possible to simply pump on the CdS loaded zeolite and remove all of the sulfur to return to a Cd zeolite given sufficient time. We believe that equilibrium (5) is the basic reason for the breaking up of superclusters and the presence of defects. One way to improve the quality of the supercluster is to monitor the Cd/S ratio *in situ* during the growth process, and to find optimal growth conditions such as temperature, flow

rate, etc. In essence, one needs the kind of precise control that are characteristic of modern epitaxial growth techniques. With respect to the in situ monitoring of Cd/S ratio, we have done thermogravimetric analysis of a sample loaded with a 5 fold excess of $H_2S$ over that necessary to completely convert all Cd sites to CdS. The data shows that all $H_2S$ are removed smoothly by flushing with nitrogen so that no break in the weight loss curve corresponding to the 1:1 Cd:S stoichiometry is apparent. This makes the monitoring and control of Cd/S ratio difficult and the empirical trial and error approach is more or less needed.

To avoid the problems associated with equilibrium (5) and to bypass the inherent limitation of the ion-exchange method in terms of loading capability, alternative organometallic synthetic routes may be needed. As we mentioned before, a major reason for the inhomogenity of supercluster size distribution is due to the partial vacancy of the sodalite cages, which in turn originates from the limited ion-exchange capability of zeolites. With zeolite 13 X, which has the highest ion-exchange capability, the highest CdS loading achieved is 25 wt% which is close to the 27 wt% level needed for full occupancy of all sodalite cages. An organometallic route is also necessary if one wants to fill up the supercages which would yield superclusters with totally different structures and electronic properties. We are currently exploring these alternative approaches.


## V. SUMMARY:

Well-defined CdS clusters and superclusters have been synthesized within the pore structure of zeolite Y. At low CdS loading density,

$(CdS)_{1-4}$ clusters are formed inside the sodalite cages. Their absorption spectra have a shoulder near 290 nm. At high loading density, discrete $(CdS)_4$ cubes begin to interconnect to form a supercluster (or superlattice) structure. The absorption spectrum of the supercluster has a shoulder near 350 nm. The discrete $(CdS)_4$ cube building blocks consist of interlocking tetrahedra of Cd and S with a Cd-S bond length of 2.47Å. A supercluster then consists of many such interconnected $(CdS)_4$ cubes with spatial geometry defined by that of the sodalite units. In zeolite Y, cubes in the adjacent sodalite units have Cd atoms pointing toward each other through the double 6-ring window with a Cd-Cd distance of ~ 6Å.

The unique stability of $(CdS)_4$ clusters inside the sodalite units is due to the coordination of Cd atoms with the framework oxygen atoms of the double 6-ring windows. The stability of the supercluster comes from the interaction between $(CdS)_4$ clusters in the adjacent sodalite units. We suggest that through-bond coupling is responsible for the interaction between $(CdS)_4$ clusters.

Semiconductor superclusters represent a novel class of materials where the 3-dimensional structure and electronic properties can be controlled by using different zeolites as the template. Imperfections do exist with these materials at present. Alternative synthetic routes and better control in fabrication processes need to be explored in the future. Large single crystal zeolites are required for exploring the optoelectronic properties.

## ACKNOWLEDGEMENTS.

# REFERENCES

1.  Kroto, H. W.; Heath, J. R.; O'Brien, S. C.; Curl, R. F. and Smalley, R. E., *Nature*, **1985**, 318, 162.

2.  Rohlfing, E. A.; Cox, D. M. and Kaldor, A., *Chem. Phys. Lett.*, **1983**, 99, 161.

3.  Riley, S. J.; Parks, E. K.; Mao, L.; Pobo, G.; and Wexler, S., *J. Phys. Chem.*, **1982**, 86, 3911.

4.  a.  Lucas, M., *Bull. Soc. Chim.*, **1896**, (3), 15, 40.

    b.  Ewan, T., *J. Soc. Chem. Ind.*, **1909**, 10, 10.

5.  Berry, C. R., *Phys. Rev.*, **1967**, 161, 848.

6.  a.  Brus, L. E., *J. Phys.Chem.*, **1986**, 90, 2555 and references therein.

    b.  Brus, L. E., *J. Chem. Phys.*, **1984**, 80, 4403.

    c.  Rossetti, R.; Hull, R.; Gibson, J. M. and Brus, L. E., *J. Chem. Phys.*, **1985**, 83, 1406.

7.  Weller, H.; Schmidt, H. M.; Koch, U.; Fojtik, A.; Baral, S.; Henglein, A; Kunath, W.; Weiss, K. and Dieman, E., *Chem. Phys. Lett.*, **1986**, 124, 557, and references therein.

8.  a.  Nozik, A. J.; Williams, F.; Nenadovic, M. T.; Rajh, T. and Micic, O. I., *J. Phys. Chem.*, **1985**, 89, 397.

    b.  Nedeljkovic, J. M.; Nenadovic, M. T.; Micic, O. I. and Nozik, A. J., *J. Phys. Chem.*, **1986**, 90, 12.

9.  Ramsden, J. J.; Webber, S. E. and Gratzel, M., *J. Phys. Chem.*, **1985**, 89, 2740.

10. Tricot, Y-M. and Fendler, J. H., *J. Phys. Chem.*, **1986**, <u>90</u>, 3369.

11. a. Sandroff, C. J.; Hwang, D. M. and Chung, W. M., *Phys. Rev. B*, **1986**, <u>33</u>, 5953.

    b. Sandroff, C. J. and Farrow, L. A., *Chem. Phys. Lett.*, **1986**, <u>130</u>, 458.

    c. Sandroff, C. J.; Kelty, S. P. and Hwang, D. M., *J. Chem. Phys.*, **1986**, <u>85</u>, 5337.

12. Dannhauser, T.; O'Neil, M.; Johansson, K.; Whitten, D. and McLendon, G., *J. Phys. Chem.*, **1986**, <u>90</u>, 6074.

13. a. Ekimov, A. I. and Onushchenko, A. A., *JETP Lett.*, **1984**, <u>40</u>, 1136.

    b. Ekimov, A. I.; Efros, Al. L. and Onushchenko, A. A., *Solid State Comm.*, **1985**, <u>56</u>, 921.

    c. Efros, Al. L. and Efros, A. L., *Sov. Phys. Semicond.*, **1982**, <u>16</u>, 772.

14. Borrelli, N. F.; Hall, D. W.; Holland, H. J. and Smith, D. W., *J. Appl. Phys.*, **1987**, <u>61</u>, 5399.

15. Wang, Y. and Mahler, W., *Opt. Comm.*, **1987**, <u>61</u>, 233.

16. Wang, Y.; Suna, A.; Mahler, W. and Kasowski, R., accepted for publication in *J. Chem. Phys.*

17. Teo, Boon K.; Keating, K. and Kao, Y.-H., *J. Am. Chem. Soc.*, **1987**, <u>109</u>, 3494.

18. Baker, M.; Godber, J. and Ozin, G. A., *J. Phys. Chem.*, **1985**, <u>89</u>, 2299.

19. Wang, Y. and Herron, N., *J. Phys. Chem.*, **1987**, <u>91</u>, 257.

20. Parise, J. B.; Mac Dougall, J.; Herron, N.; Farlee, R.; Sleight, A. W.; Wang, Y.; Bein, T.; Moller, K. and Moroney, L.M., submitted for publication.

21.     Wang, Y. and Herron, N., in print, *J. Phys. Chem.*, September issue,1987.

22.     "Reflectance Spectroscopy", G. Kortum, Springer-Verlag, New York,1969.

23.     Grum, F. and Wightman, T. E., *Applied Optics*, **1977**, 16, 2775.

24.     Patterson, E. M.; Shelden, C. E. and Stockton, B. H., *Applied Optics*, **1977**, 16, 729.

25.     x13A beam line

26.     Lee, P. A.; Citrin, P. H.; Eisenberger, P and Kincaid, B. M., *Rev. of Modern Physics*, **1981**, 53, 769.

27.     Wasser, J.; Levy, H. A. and Peterson, S. W., *Acta Cryst.*, **1953**, 6, 661.

28.     Matkovic, B.; Ribar, B.; Zelenko, B. and Peterson, S., *Acta Cryst.*, **1966**, 21, 719.

29.     Wyckhoff, R. W. G., "Crystal Structures", 2nd ed.,        Interscience, 1963

30.     Kirkpatrick, S., *Rev. Mod. Phys.*, **1973**, **45**, 574; and references therein.

31.     Saunders, M. J.; Catlow, C. R. A., *Int. Zeol. Conf., Reno, NV*, **1984**.

32.     Calligaris, M.; Mardin, G.; Randaccio, L. and Zangrando, E., *Zeolites*, **1986**, 6, 439.

33.     Costenoble, M. L.; Mortier, W. J. and Uytterhoeven, J. B., *J. Chem. Soc., Faraday Trans. 1*, **1978**, 74, 466.

34.     Strukturberichte, Vol., 1, 1923/28, 72.

35.     "Landolt-Bornstein, New Series", Vol. 17, subvol. b, edited by O.Madelung, Springer-Verlag, New York, 1983.

36. Many previous attempts to prepare and study the spectrum of CdS molecules in gas phase have failed due to their extreme instability. See "Constants of Diatomic Molecules" by Huber, K. P.; Herzberg, G. Van Nostrand Reinhold Company, 1979.

37. Karge, H. G.; Ziolek, M. and Laniecki, M., *Zeolites*, **1987**, 7, 197.

38. "Thin Films: Preparation and Properties" Tu, K. N. and Rosenberg, R., Eds. New York, Academic, 1983.

39. Hoffmann, R.; Imamura, A. and Hehre, W. J., *J. Am. Chem. Soc.*, **1968**, 90, 1499.

40. Paddon-Row, M. N., *Acc. Chem. Res.*, **1982**, 15, 245.

41. Herman, A.; Dreczewski, B. and Wojnowski, W., *Chem. Phys.*, **1985**, 98, 475.

## Figure Captions

**Figure 1.**  Representations of the tetrahedral atom framework of zeolites which depict the tetrahedral T atoms (T=Si or Al) as connected points. In this depiction oxygen atoms have been omitted but would lie approximately midway between the T atoms.  a) orthographic pair view of zeolite Y or X ;b) zeolite A.

**Figure 2.**  IR spectra (nujol mull) of: a) zeolite NaY (hydrated), b) $Cd^{2+}$ ion exchanged Y (dehydrated), and c) CdS in zeolite Y.

**Figure 3.**  Scattering coefficients of zeolite Y and M.

**Figure 4.**  Absorption spectra of CdS in zeolite Y compared to that of micron size CdS powder and the calculated Lorenz-Mie spectrum (with medium dielectric constant assumed to be 30).  The low-loading sample contains 1.1wt% CdS and the high loading sample contains 7.4 wt% CdS.  The absorption coefficients are normalized to the volume concentration of CdS.

**Figure 5.**  Absorption spectra of CdS in zeolite Y as a function of CdS concentrations:  7.4 wt%, 6.53 wt%, and 5.86 wt%.

**Figure 6.**  The excitation and emission spectra of CdS in zeolites X, Y, and A.

**Figure 7.**  The observed (dots) and calculated (solid line) x-ray powder diffractogram profiles and the difference between them for a) 18.6Cd,6.7S zeolite Y;  b) 13.5Cd,10.3S zeolite Y.

six-ring oxygen atoms (represented as points connected to T atoms by sticks) and Cd atoms of the cluster (solid circles= Cd open circles = S(O)).

**Figure 15.** The relative orientation of two CdS clusters in adjacent sodalite units of the Y structure separated by a double six-ring linkage. (solid circles = Cd; open circles = S(O)) Cubes are viewed edge-on.

**Figure 16.** Relative orientation of two CdS clusters in adjacent sodalite units of the A structure separated by a double four-ring

## TABLE I

Chemical Analysis of CdS Loaded Zeolites

| Zeolites | Unit Cell Formula Calculated | wt% Cds |
|---|---|---|
| Y[a] | $Cd_{1.6}S_{4.0}Al_{56}Si_{136}$ | 1.0% |
| Y | $Cd_{1.41}S_{1.41}Al_{56}Si_{136}$ | 1.09% |
| Y | $Cd_{2.3}S_{4.1}Al_{56}Si_{136}$ | 1.8% |
| Y | $Cd_{3.1}S_{4.5}Al_{56}Si_{136}$ | 3.0% |
| Y | $Cd_{5.5}S_{4.6}Al_{56}Si_{136}$ | 5.4% |
| Y | $Cd_{5.8}S_{5.0}Al_{56}Si_{136}$ | 5.9% |
| Y | $Cd_{6.2}S_{4.8}Al_{56}Si_{136}$ | 6.0% |
| Y | $Cd_{10.4}S_{11.0}Al_{56}Si_{136}$ | 11.3% |
| Y | $Cd_{13.4}S_{14.6}Al_{56}Si_{136}$ | 11.8% |
| Y | $Cd_{13.5}S_{10.3}Al_{56}Si_{136}$ | 13.0% |
| Y | $Cd_{15.9}S_{17.1}Al_{56}Si_{136}$ | 15.6% |
| Y | $Cd_{18.6}S_{6.7}Al_{56}Si_{136}$ | 16.0% |
| Y | $Cd_{22.6}S_{24}Al_{56}Si_{136}$ | 18.2% |
| X[a] | $Cd_{21.0}S_{14.0}Al_{90}Si_{102}$ | 18.8% |
| X | $Cd_{29.1}S_{30.0}Al_{86}Si_{106}$ | 24.8% |
| A[b] | $Cd_{2.3}S_{2.6}Al_{12}Si_{12}$ | 17.0% |
| A | $Cd_{4.0}S_{3.3}Al_{12}Si_{12}$ | 25.6% |

a. 8 sodalite units/unit cell
b. 1 sodalite unit/unit cell

## TABLE II

### IR Absorption Bands of Zeolite Y During CdS Synthesis
### (Nujol mulls)

|  | Asymmetric Stretch | Symmetric Stretch | cm$^{-1}$ Double Rings | T-O Bend | Pore Opening |
|---|---|---|---|---|---|
| NaY (starting material) | 1130, 1005 | 784, 714, 635 | 572 | 500, 455 | 380, 260 |
| CdY (calcined) | 1145, 1040, 945 | 780, 710 635 | 580 | 450 | 380 |
| CdS/Y | 1135, 1050 955 | 780, 715 | 555 | 490, 440 | 375 |

## TABLE III

| Scatterer Pair | Bond Distance R (Å) | Coord. Number N | $N_{corr}$* | Debye-Waller $\Delta G^2$ (Å)$^2$ | Cube Model N** |
|---|---|---|---|---|---|
| **CD1** | | | | | |
| Cd-OZ | 2.44 | 2.6 | 3.0 | 0.004 | 3 |
| Cd-O/cube | 2.34 | 2.3 | 2.5 | 0.002 | 3 |
| | 2.25 | 2.2 | 2.4 | 0.0007 | |
| Cd-Si/Al | 3.42 | 9.3 | 12.4 | -0.0014 | 6 |
| Cd-Cd | 3.29 | 2.1 | 2.0 | 0.003 | 3 |
| **CD2** | | | | | |
| Cd-OZ | 2.36 | 3.1 | 3.5 | 0.004 | |
| Cd-O/cube | 2.24 | 1.7 | 1.8 | 0.0007 | |
| Cd-S//cube | | | 2.52 | 1.5 | 0.0009 |
| Cd-Si/Al | 3.42 | 9.3 | 12.4 | -0.0014 | |
| Cd-Cd | 3.29 | 2.1 | 2.0 | 0.003 | |
| **CD3** | | | | | |
| Cd-OZ | 2.44 | 2.0 | 2.3 | 0.004 | |
| Cd-O/cube | 2.32 | 1.7 | 1.9 | 0.004 | |
| | 2.23 | 2.2 | 2.4 | 0.0009 | |
| Cd-S/cube | 2.52 | 1.0 | | 0.001 | |
| Cd-Si/Al | 3.40 | 6.7 | 8.9 | 0.0009 | |

*coordination numbers corrected for the mean free path difference in reference and unknown

**theoretical coordination numbers for $Cd^{2+}$ when 100% are located in SI' sites, simultaneously forming a CdO cube.

## TABLE IV

### Refined Atomic and Structural Parameters
### Cd(13.5)S(10.3), and Cd(18.6)S(6.7)

space group Fd3m (International Tables I No. 227)
origin at center

|  | Cd(13.5)S(10.3) | Cd(18.6)S(6.7) |
|---|---|---|
| **T(1)** | | |
| x | -0.0536(1) | -0.0534(1) |
| y | 0.1251(1) | 0.1250(1) |
| z | 0.0359(1) | 0.0356(1) |
| B $\text{\AA}^2$ | 0.376(1) | 0.72(4) |
| | | |
| **O(1)** | | |
| x = 0.0 | | |
| y = -z | -0.1063(2) | -0.1039(2) |
| B $\text{\AA}^2$ | 1.697(2) | 2.5(2) |
| | | |
| **O(2)** | | |
| x = y | -0.0016(2) | -0.0021(3) |
| z | 0.142(3) | 0.1429(3) |
| B $\text{\AA}^2$ | 0.465(2) | 1.9(2) |
| | | |
| **O(3)** | | |
| x = y | 0.0748(2) | 0.0753(2) |
| z | -0.0314(4) | -0.0305(3) |
| B $\text{\AA}^2$ | 0.667(3) | 1.0(2) |
| | | |
| **O(4)** | | |
| x = y | 0.0725(2) | 0.0737(2) |
| z | 0.3215(3) | 0.3223(3) |
| B $\text{\AA}^2$ | 1.224(2) | 1.0(2) |
| | | |
| **Na(1)** | | |
| x = y = z | 0.0 | |
| | 1.8(2) | 3.3(2) |
| occ. | | |

| | | |
|---|---|---|
| **Na(2)** | | |
| x = y = z | 0.040(3) | |
| occ. | 2.9(4) | |
| **Na(3)** | | |
| x = y = z | 0.2391(4) | 0.2453(6) |
| occ. | 13.4(4) | 9.2(2) |
| **Cd(4)** | | |
| x | 0.4222(7) | 0.4220(6) |
| y | 0.2220(7) | 0.2116(6) |
| z | 0.1819(7) | 0.1808(7) |
| occ | 4.1(2) | 8.3(2) |
| **Cd(1)** | | |
| x = y = z | 0.0686(2) | 0.0702(1) |
| **S(1)** | | |
| x = y = z | 0.1654(4) | 0.1685(4) |
| occ. | 23.8(8) | 30.3(8) |
| **O(5)** | | |
| x = y = z | 0.139(3) | 0.136(2) |
| occ. | 3.8(4) | 1.5(2) |
| **O(6)** | | |
| x | 0.133(3) | 0.105(4) |
| y | 0.481(2) | 0.455(2) |
| z | 0.091(3) | 0.109(3) |
| occ. | 15.2(9) | 13.2(8) |
| **O(7)** | | |
| x | 0.097(2) | 0.091(1) |
| y | 0.024(2) | 0.003(2) |
| z | 0.482(2) | 0.467(2) |
| occ. | 17.5(13) | 22.4(12) |
| a = b = c Å | 24.6627(4) | 24.6080(2) |

| | | |
|---|---|---|
| zeropt | 2.10(4) | 1.94(3) |
| $U$ | 1223(60) | 352(20) |
| $V$ | -449(32) | -247(18) |
| $W$ | 92(5) | 70(4) |
| $X$ | 5.9(9) | 1.2(5) |
| $Y$ | 4.1(2) | 4.6(2) |
| $R_n$ | 9.3% | 10.5% |
| $R_{pr}$ | 21.2% | 21.3% |
| $R_{wpr}$ | 21.6% | 22.0% |
| $R_e$ | 18.4% | 16.3% |
| $X^2$ | | |

## TABLE V

### Selected Bonds Distances (Å) and Angles (°)

|  |  |  | Cd(13.5)S(10.3) | Cd(18.6)S(6.7) |
|---|---|---|---|---|
| T(1) | -O(1) |  | 1.64 | 1.61 |
|  | -O(2) |  | 1.64 | 1.63 |
|  | -O(3) |  | 1.66 | 1.66 |
|  | -O(4) |  | 1.64 | 1.64 |
| mean |  |  | 1.643 | 1.635 |
| expected |  |  | 1.639 | 1.639 |
|  |  |  |  |  |
| O(1) | -T(1) | -O(2) | 113 | 112 |
|  |  | -O(3) | 111 | 110 |
|  |  | -O(4) | 108 | 110 |
| O(2) | -T(1) | -O(3) | 105 | 106 |
|  |  | -O(4) | 109 | 110 |
| O(3) | -T(1) | -O(4) | 111 | 109 |
|  |  |  |  |  |
| T(1) | -O(1) | -T(1) | 138 | 143 |
|  | -O(2) | - | 145 | 144 |
|  | -O(3) | - | 139 | 138 |
|  | -O(4) | - | 143 | 143 |
| Na(2) |  | -3xO(3) | 2.14 |  |
| Na(3) |  | -3xO(2) | 2.43 |  |
|  |  |  |  |  |
| Cd(1) |  | -3xO(3) | 2.48 | 2.48 |
|  |  | -O(5) | 2.28 | 2.22 |
|  |  | -S(1) | 2.45 | 2.45 |
|  |  |  |  |  |
| Cd(2) |  | -O(7) | 2.33 | 2.36 |
|  |  |  |  |  |
| O(6) |  | -O(7) |  | 2.57 |
|  |  |  |  | 2.65 |

Fig 1b
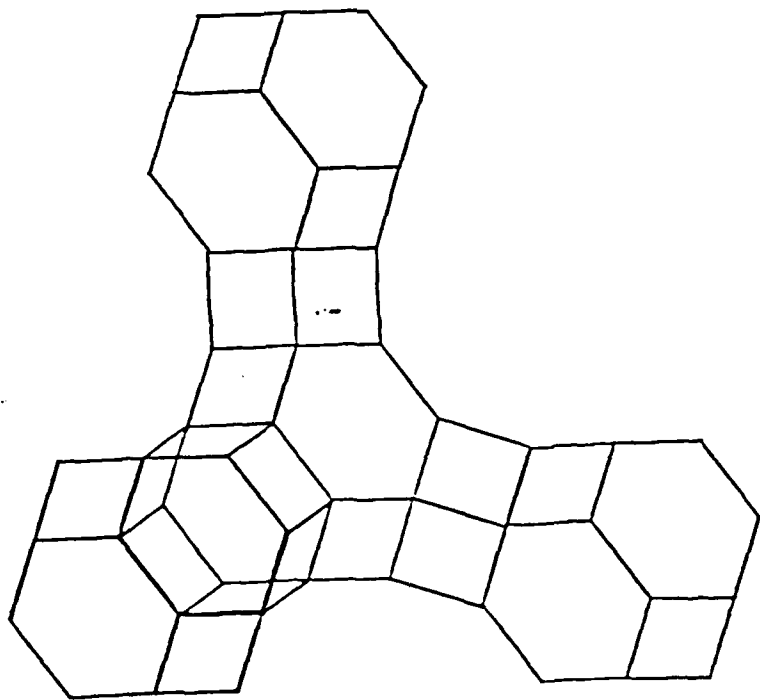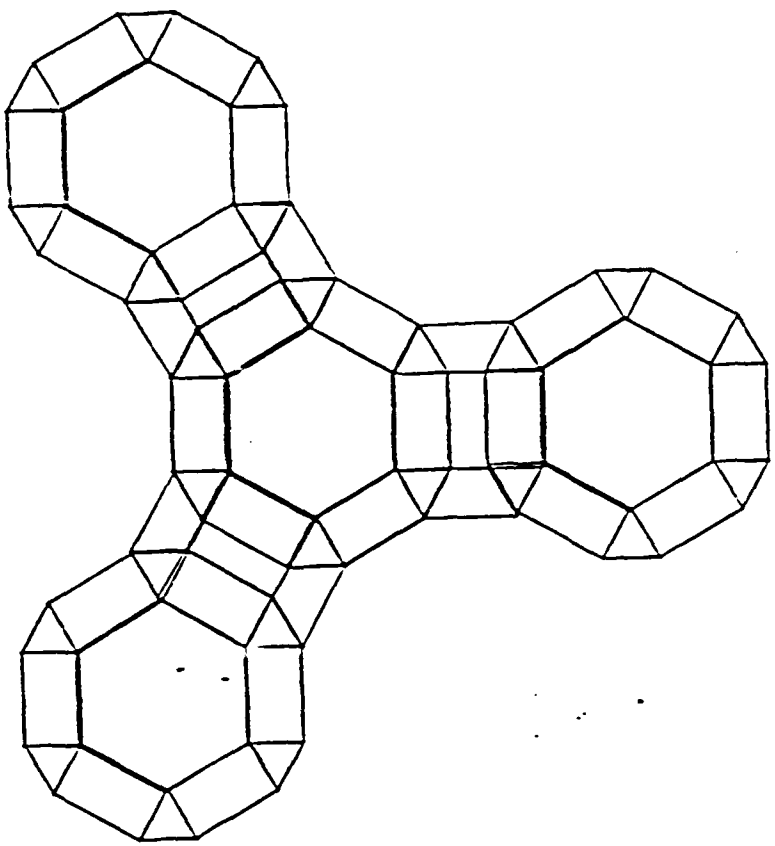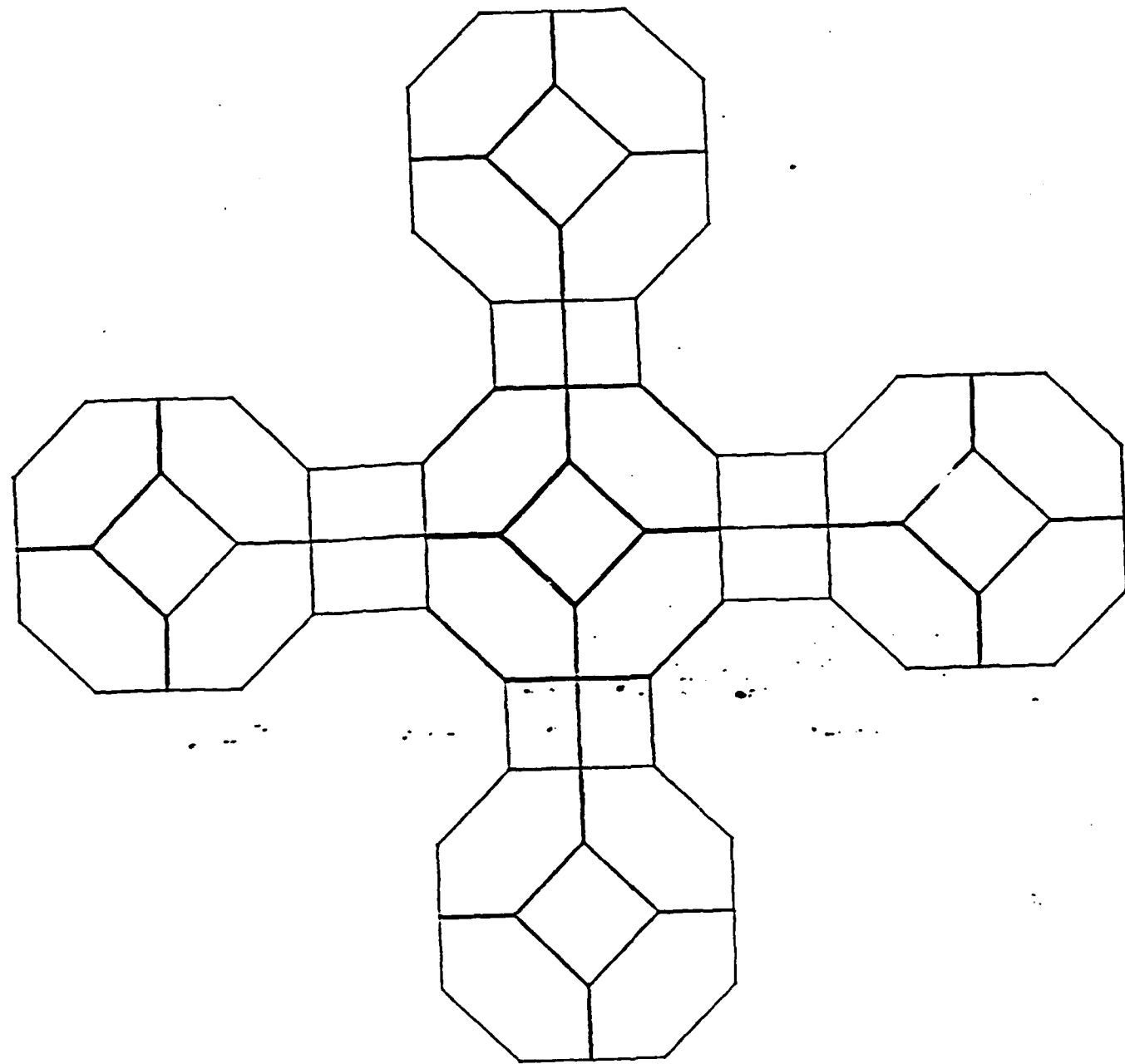
Figure 2
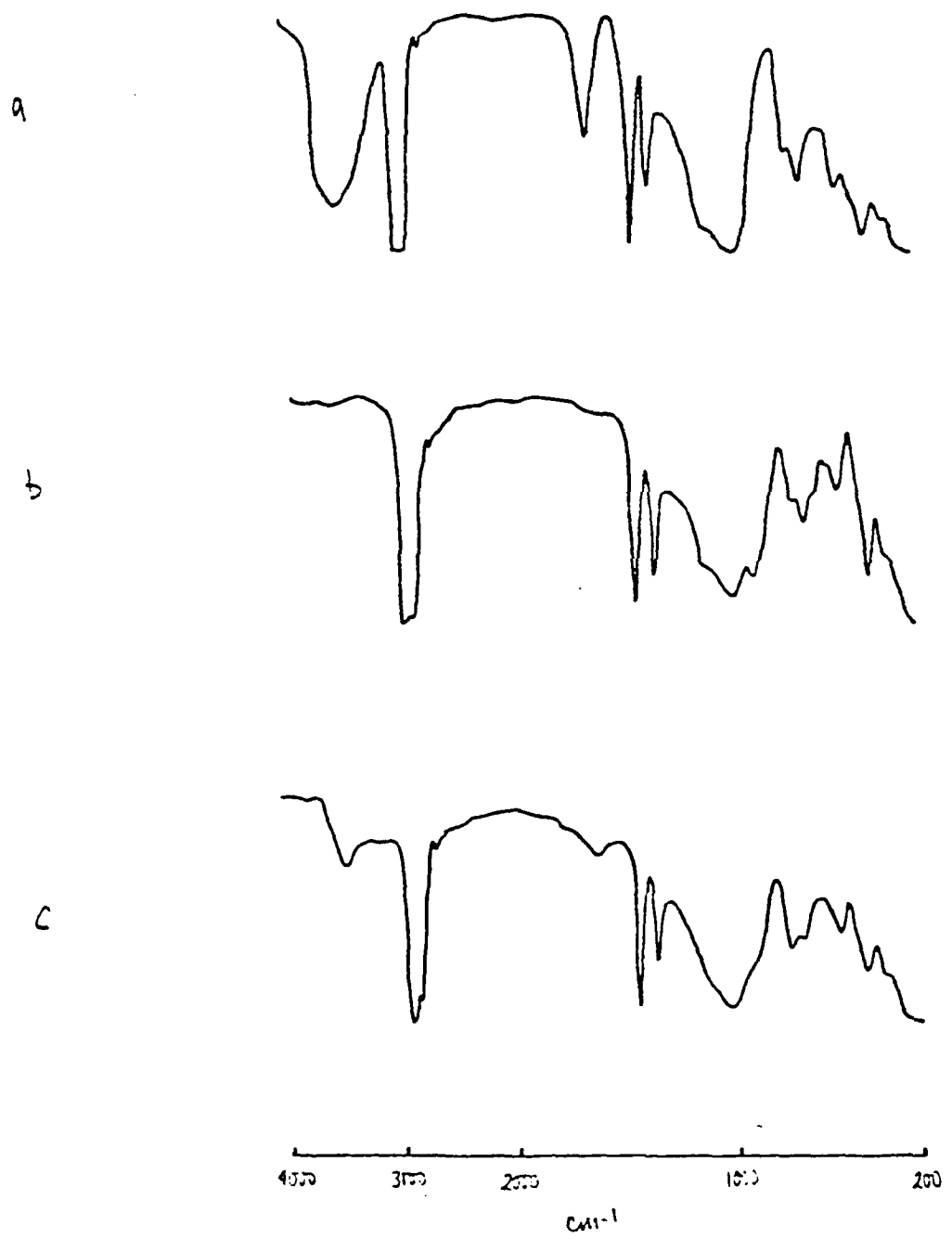


caption    IR spectra (nujol mull) of a) zeolite NaY (hydrated)   b) Cd²⁺ exchanged Y (dry) c) CdS in zeolite Y

fig 3.

scattering coefficient of zeolite M and Y

wavelength, nm

scattering coefficient

O        zeolite Y
●        zeolite M
------   565.303165*X**(-0.088979)

fig 4.2
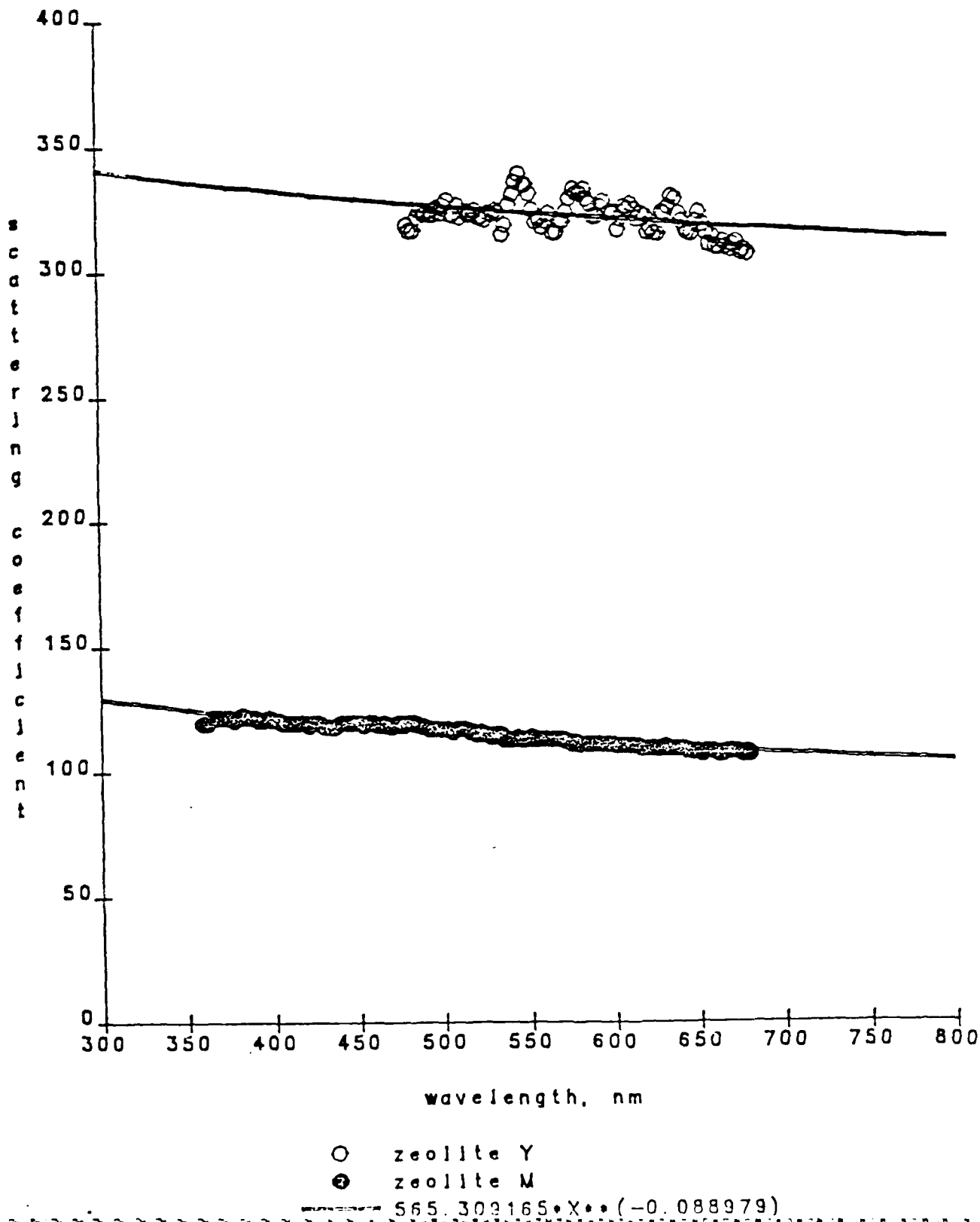


CdS/zeolite Y, quantum size effect
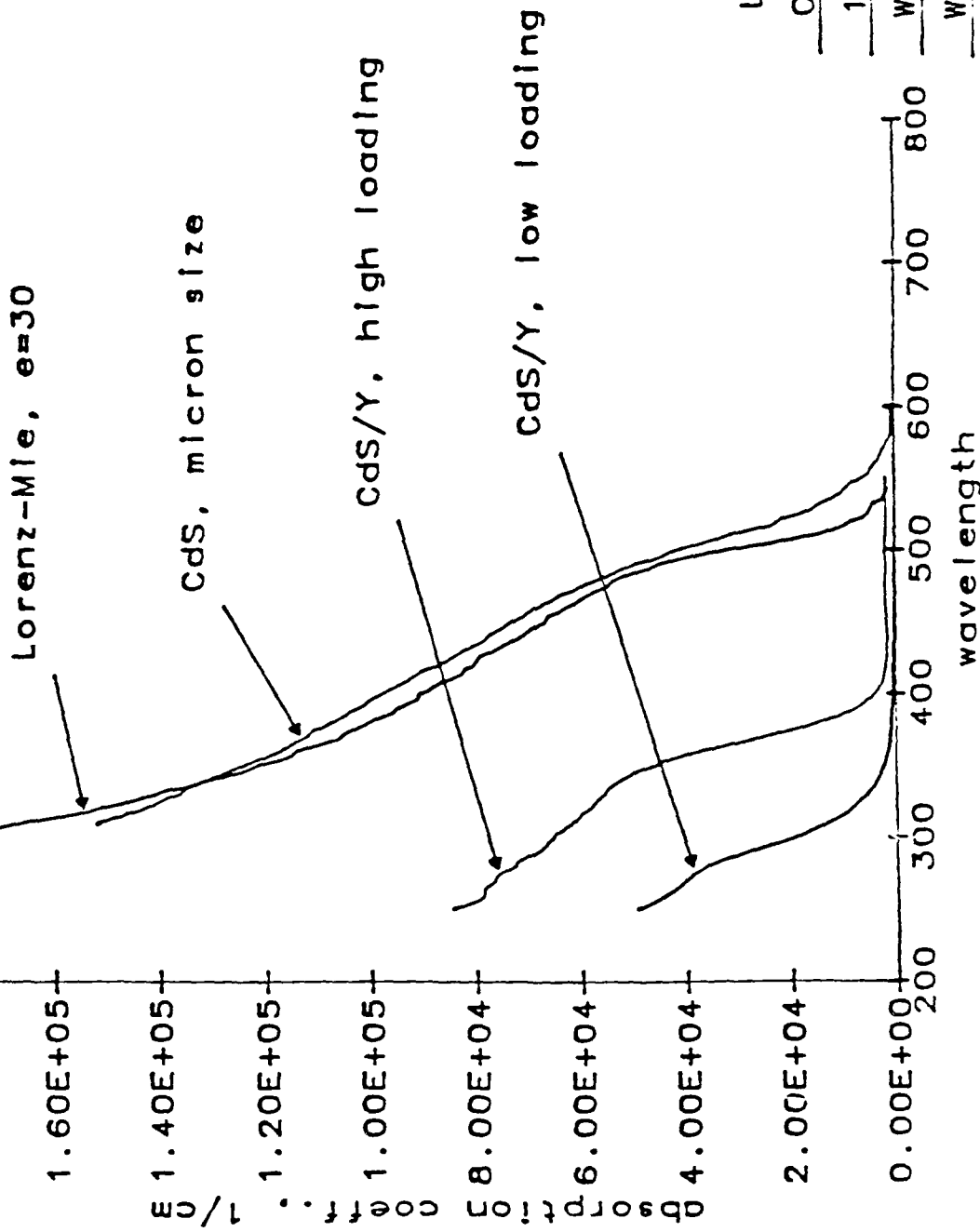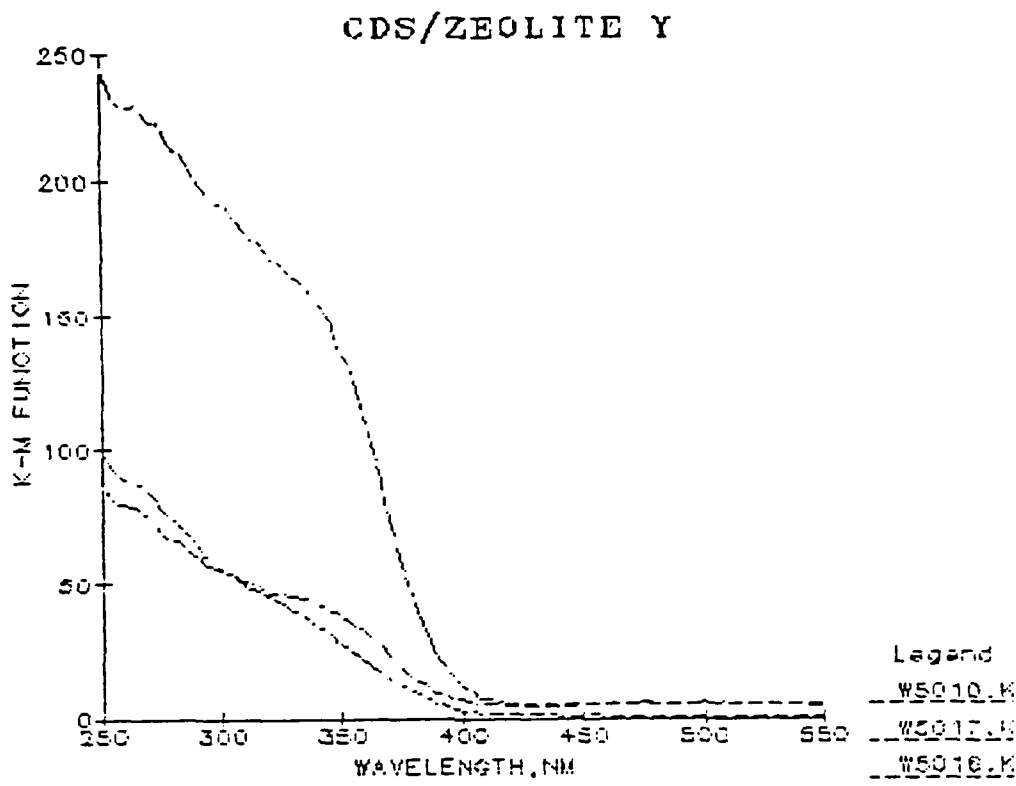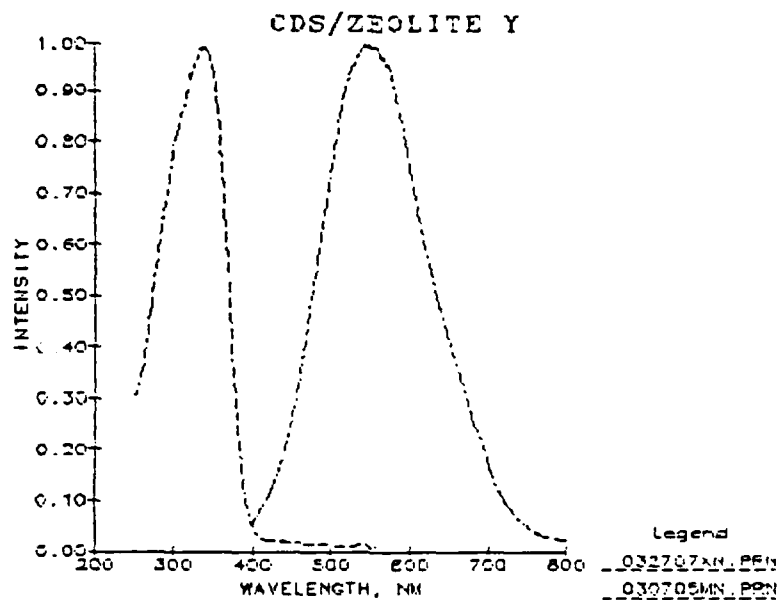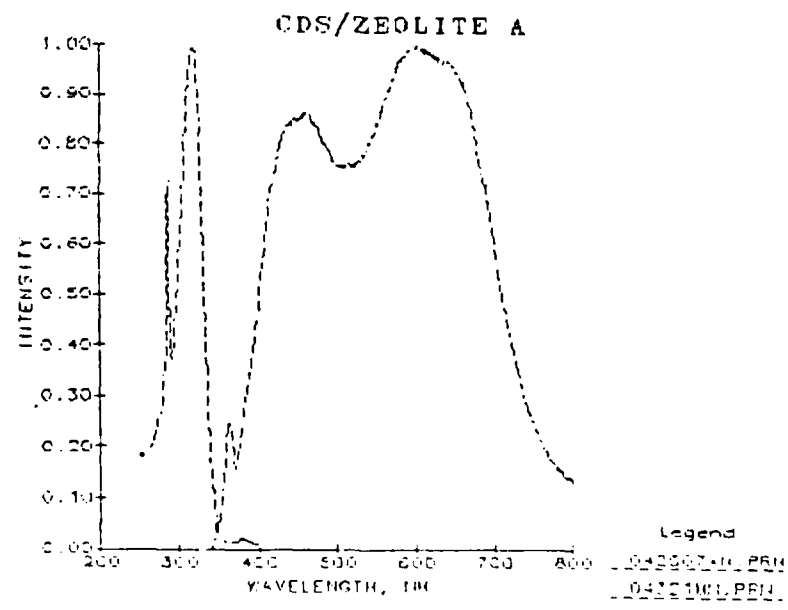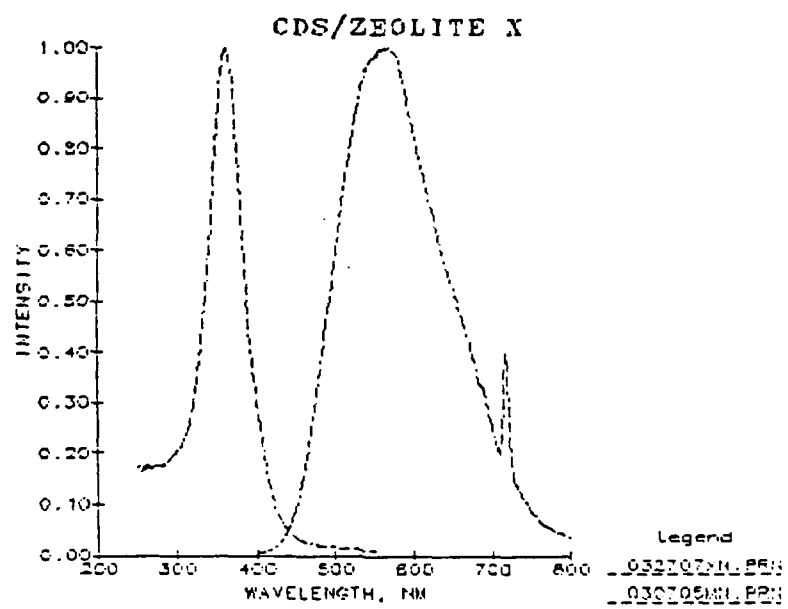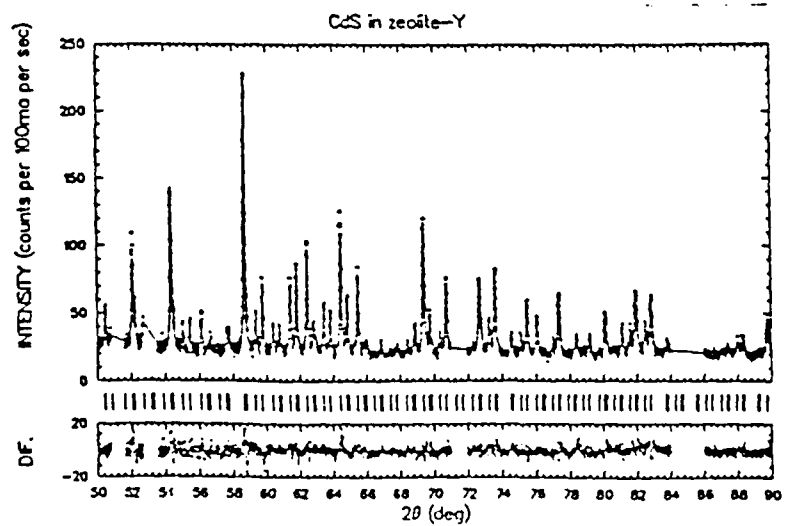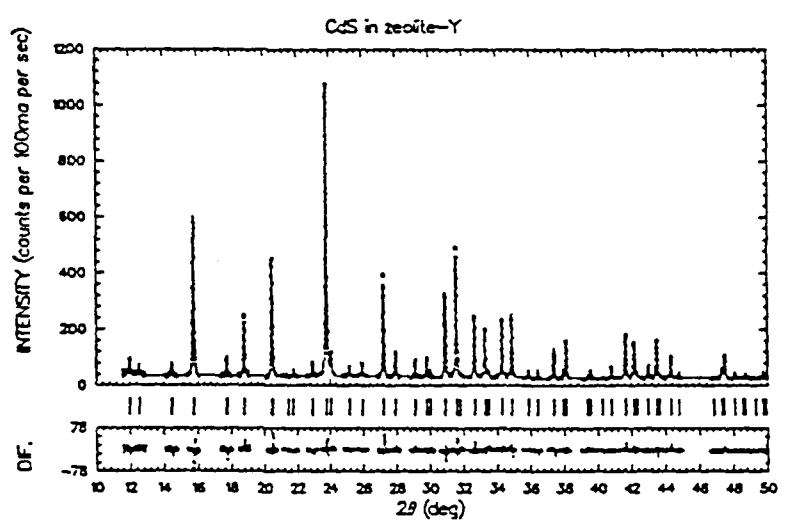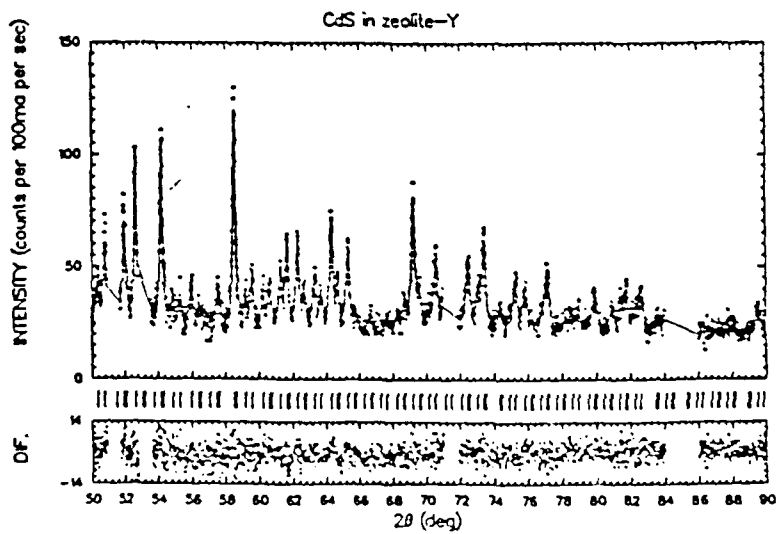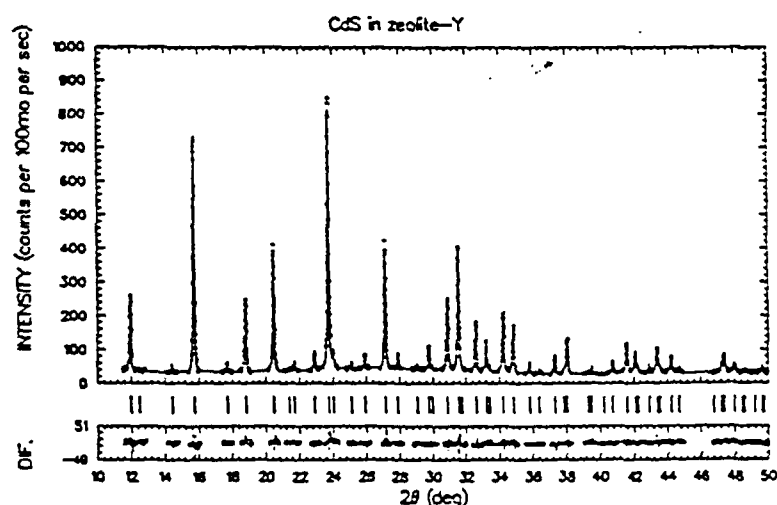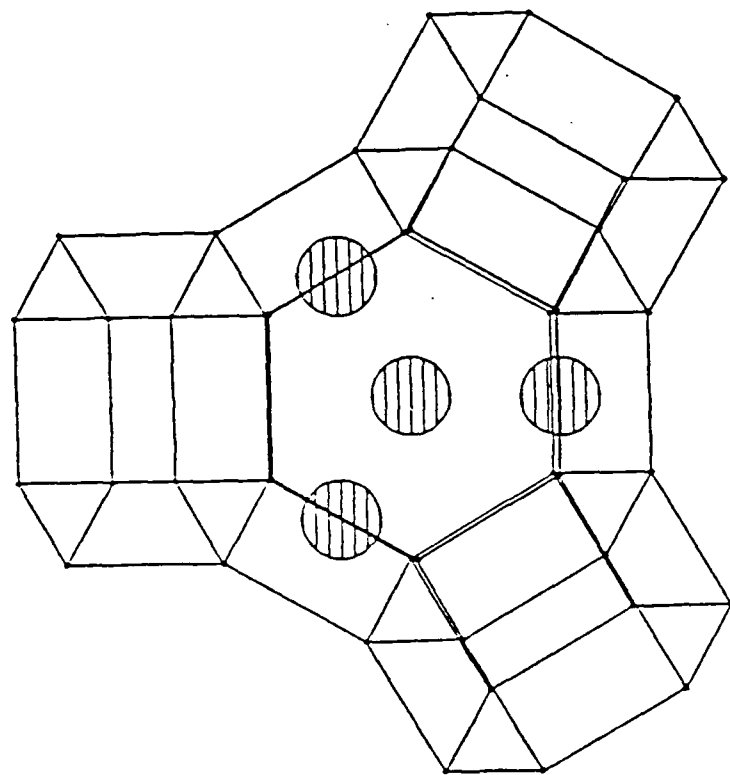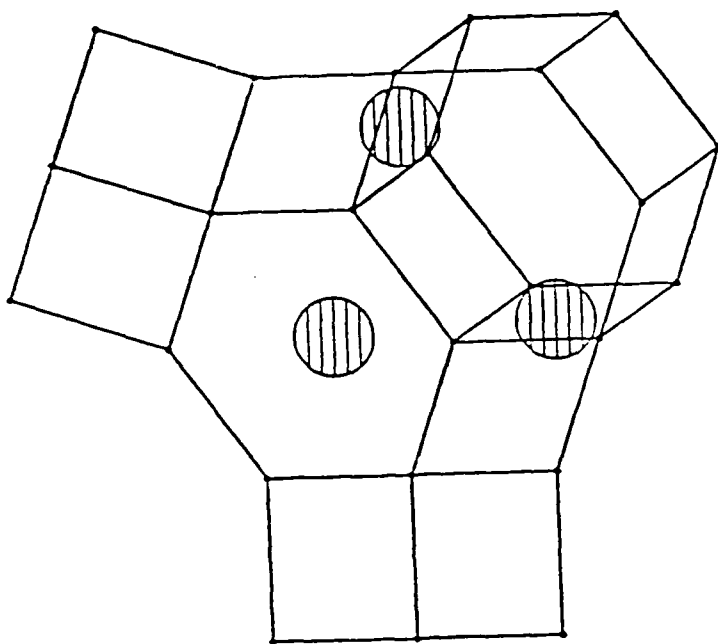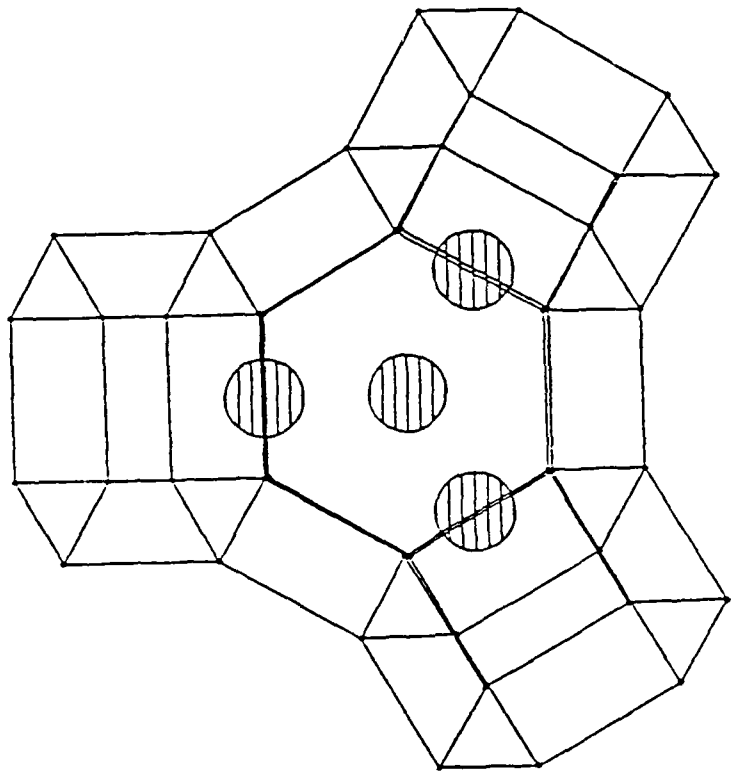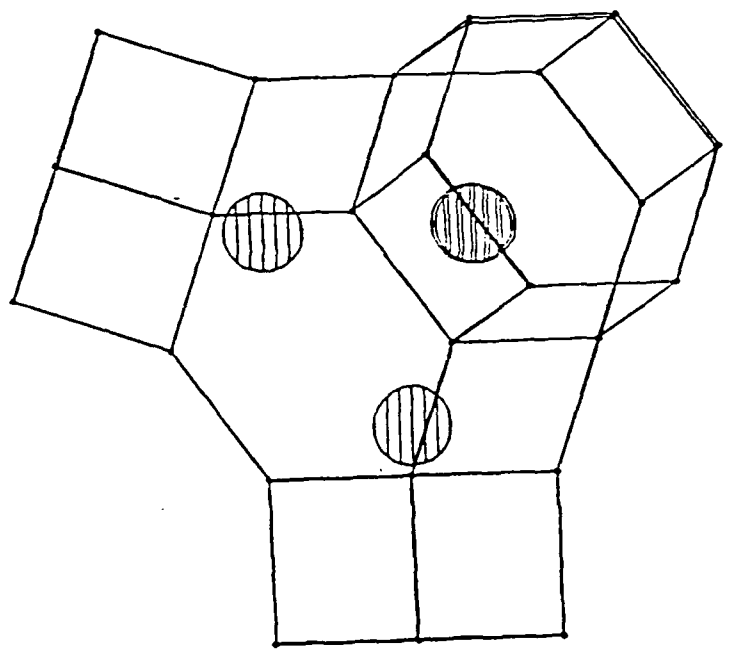
Lorenz-Mie, e=30

CdS, micron size

CdS/Y, high loading

CdS/Y, low loading

Legend
CDS3.A
120203.A
WD408.A
W5017.A

absorption coeff., 1/cm

wavelength

200   300   400   500   600   700   800

0.00E+00
2.00E+04
4.00E+04
6.00E+04
8.00E+04
1.00E+05
1.20E+05
1.40E+05
1.60E+05
1.80E+05

# CDS/ZEOLITE Y



fig 5

CDS/ZEOLITE Y

CDS/ZEOLITE X

CDS/ZEOLITE A

fig 6

fig 7(a)



CdS in zeolite-Y

CdS in zeolite-Y

fig 7(b)

CdS in zeolite-Y



CdS in zeolite-Y

Fig 8b

Fig 8.1
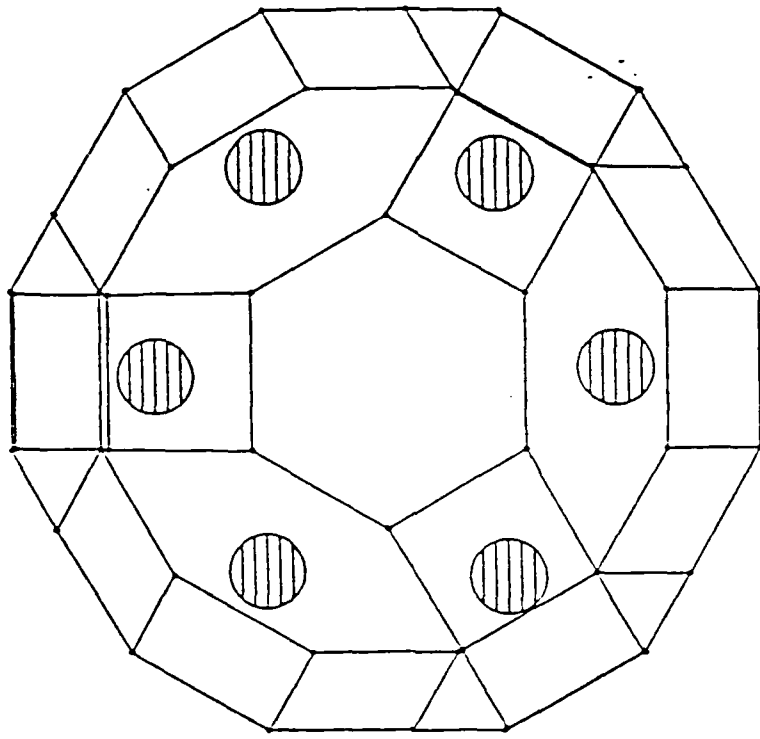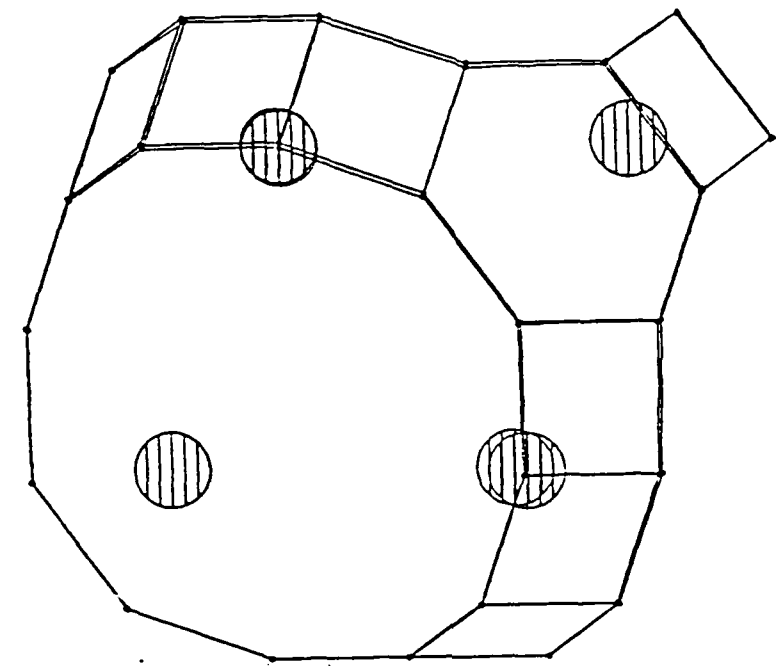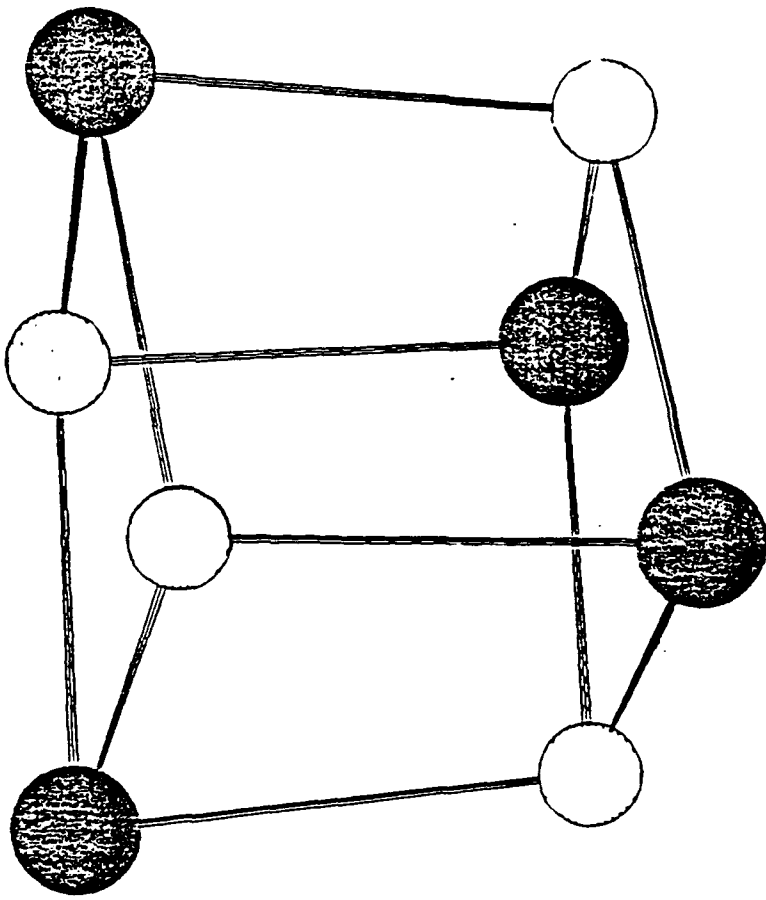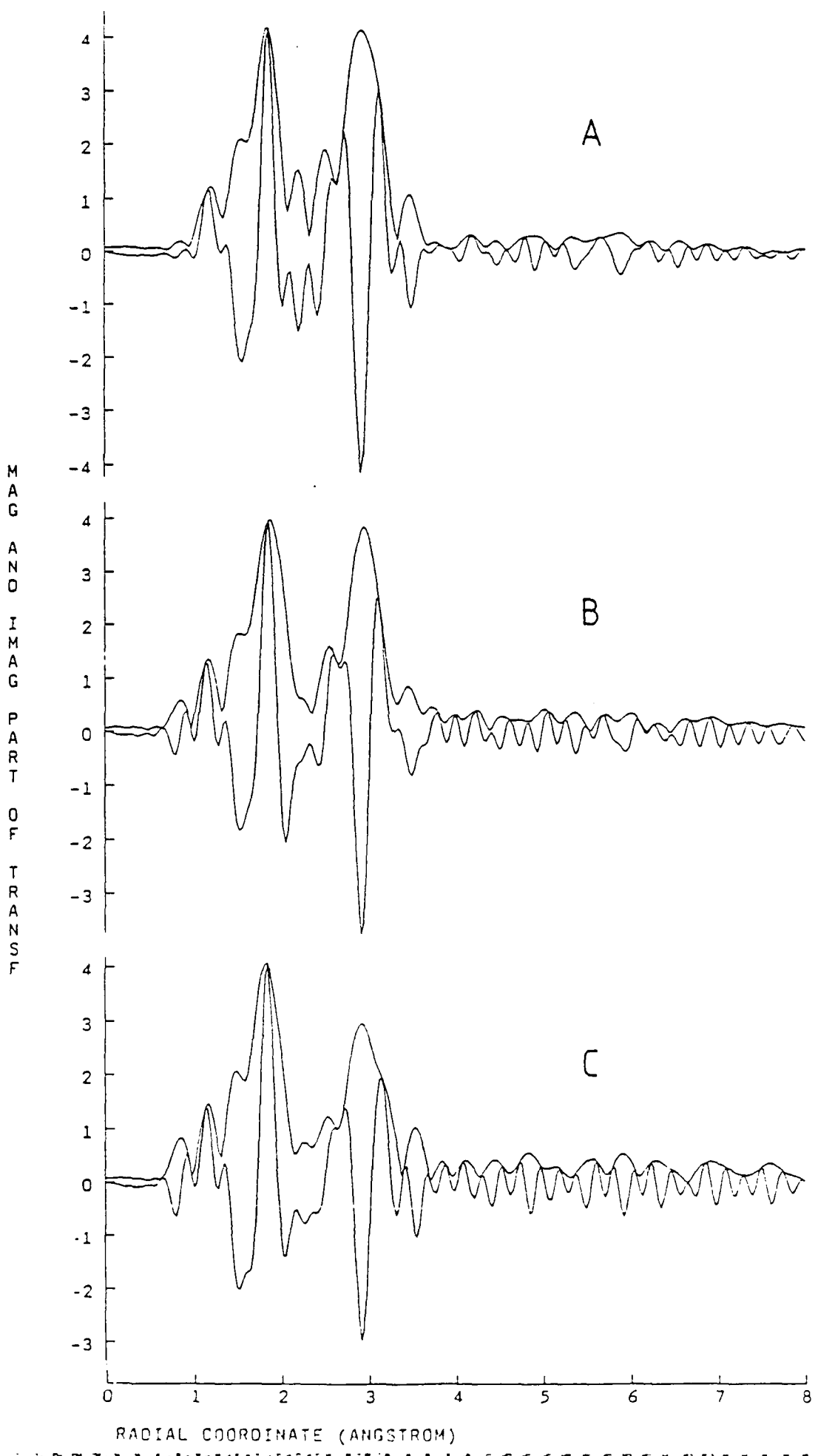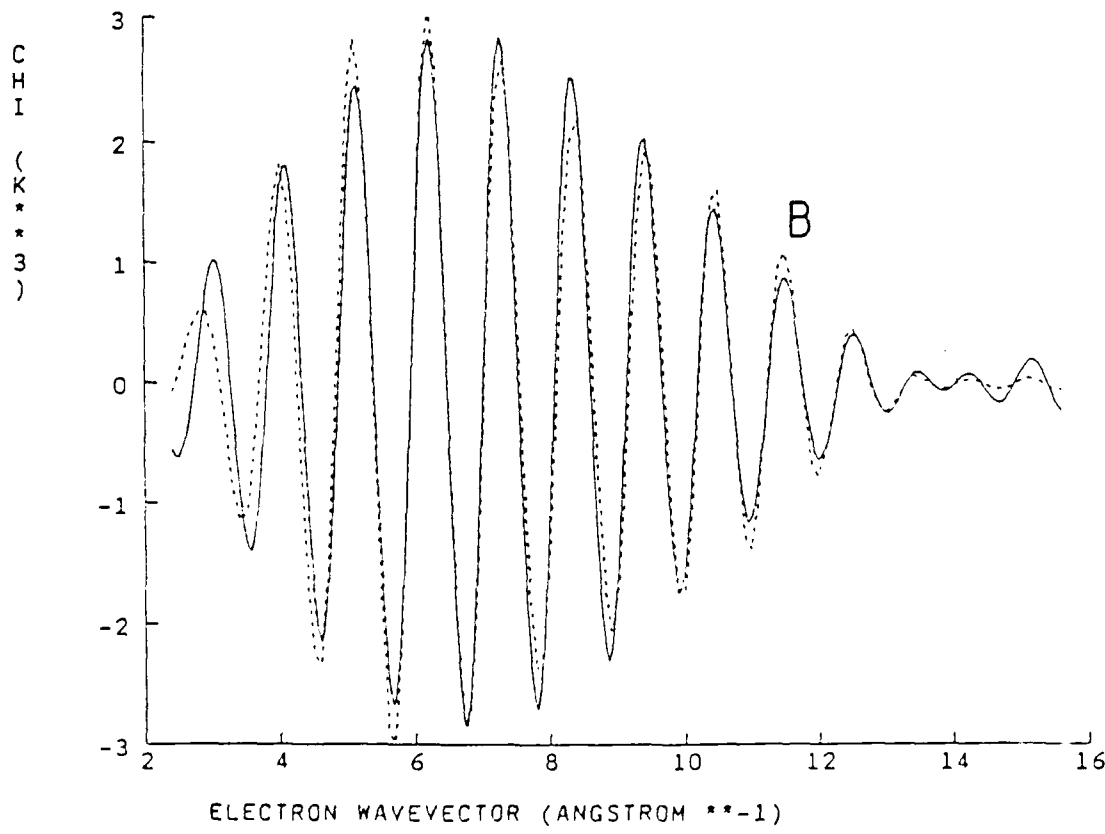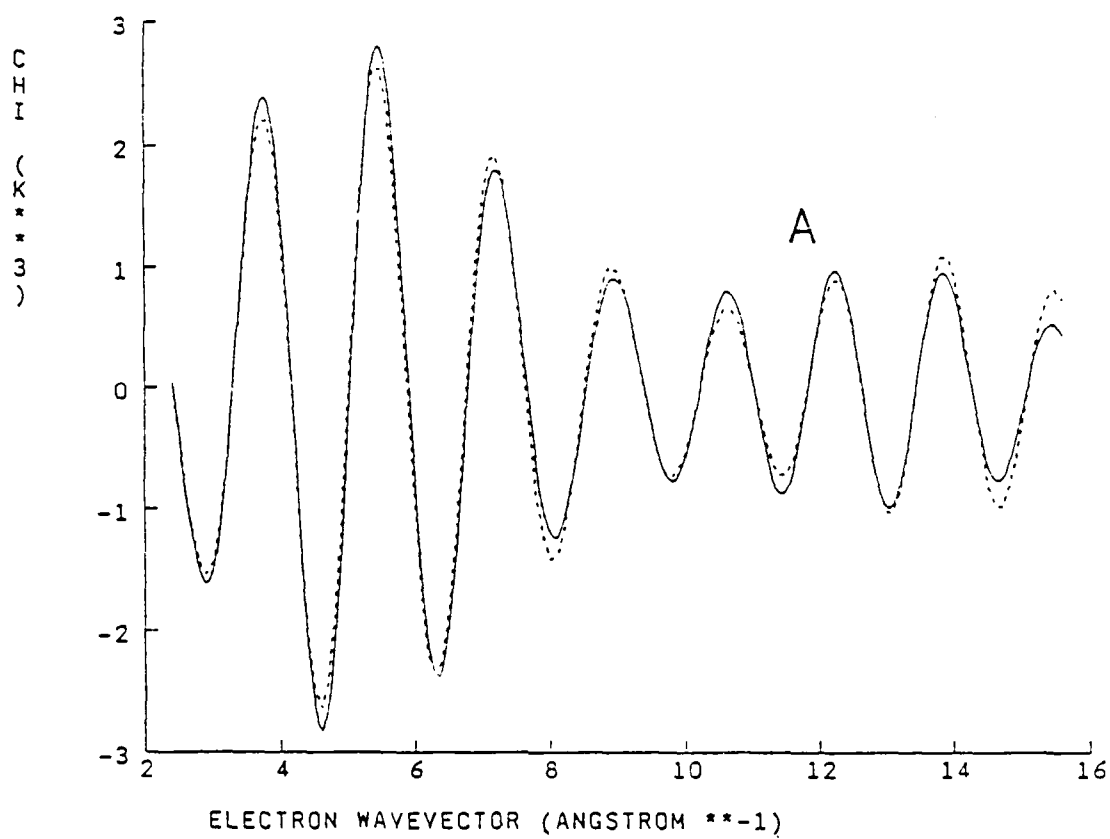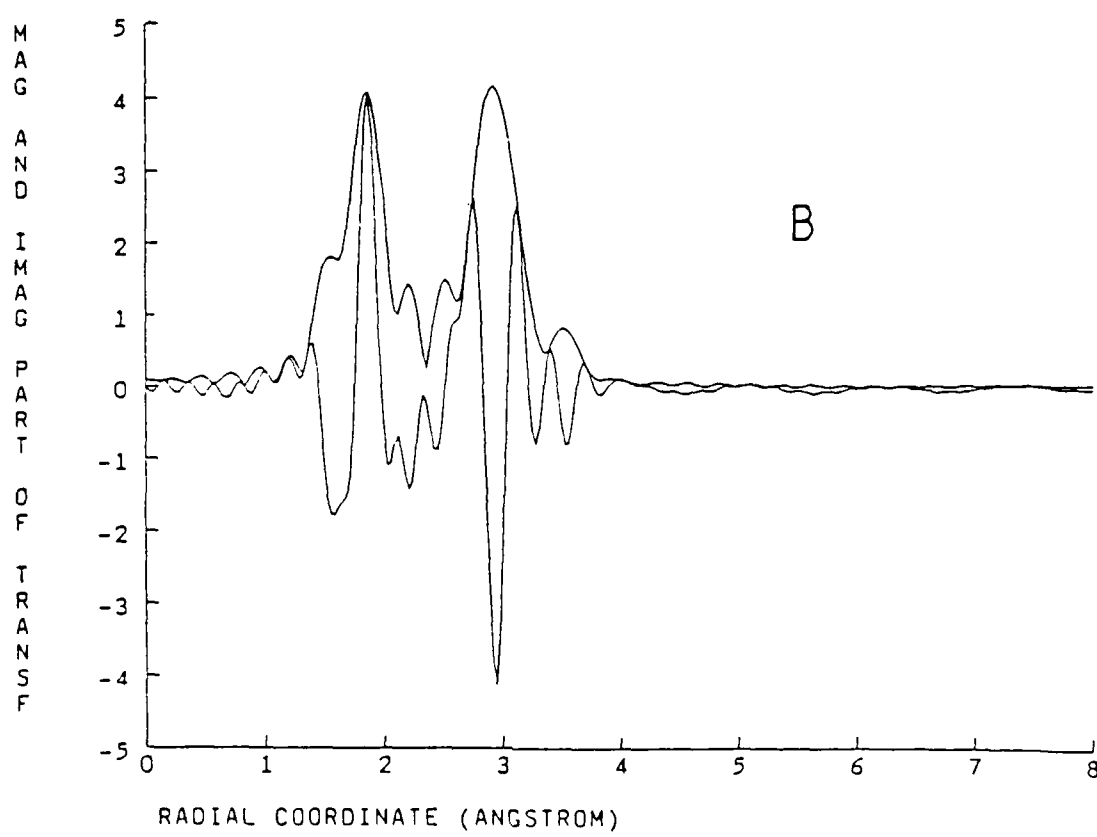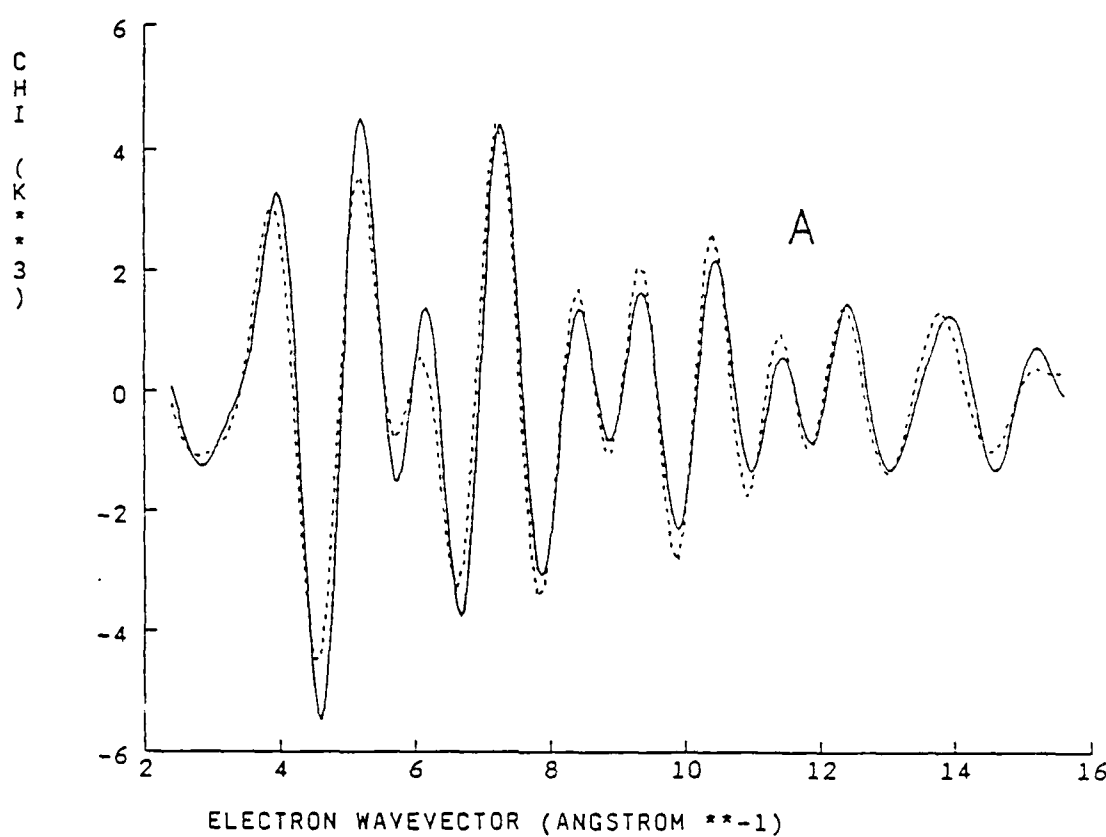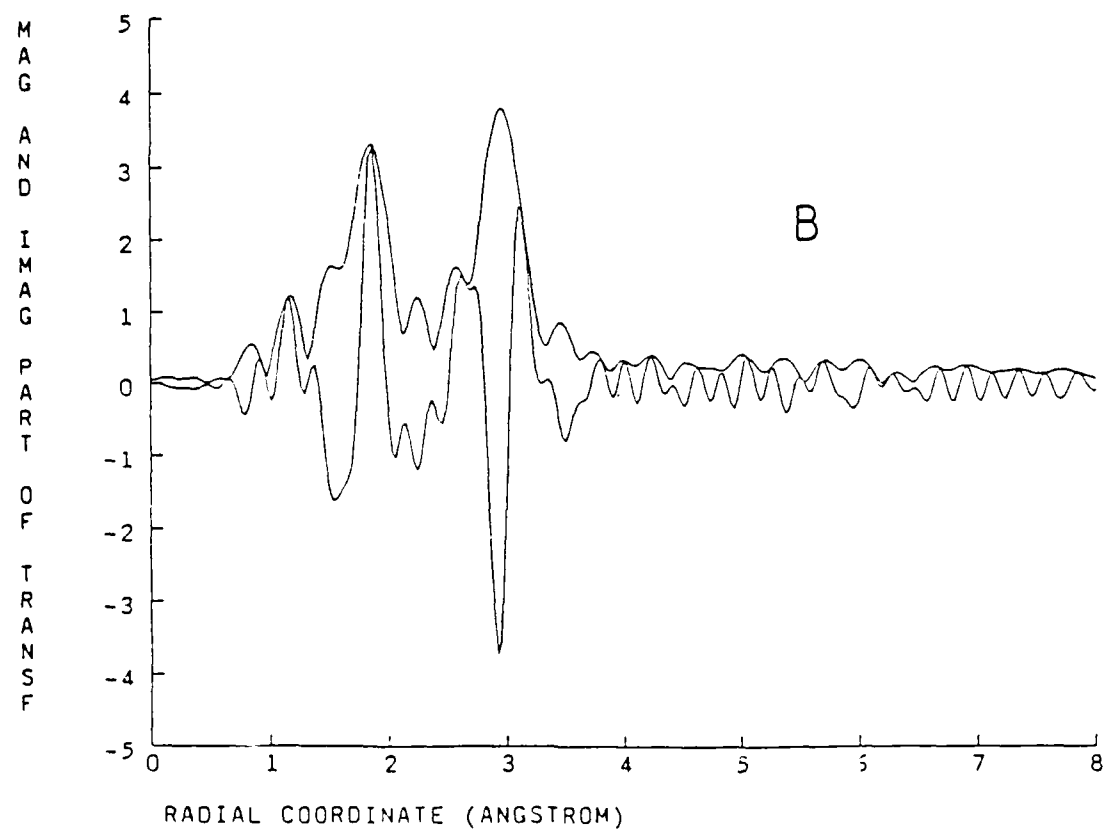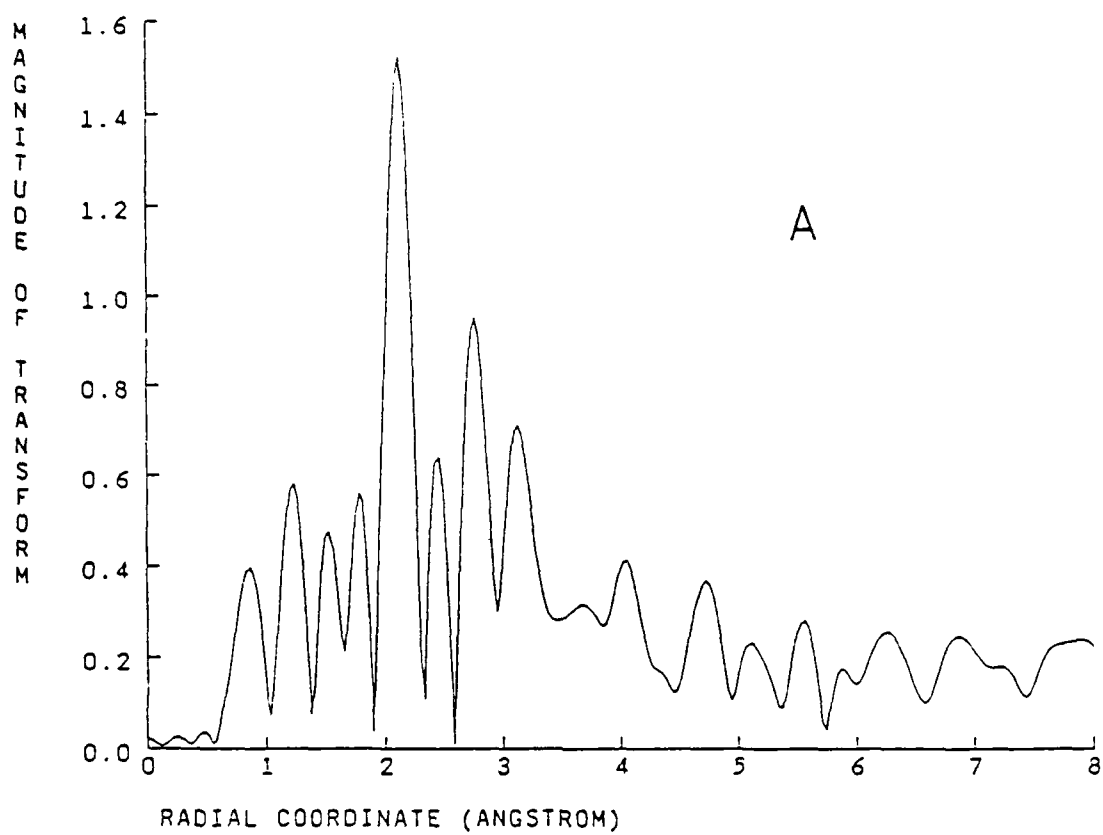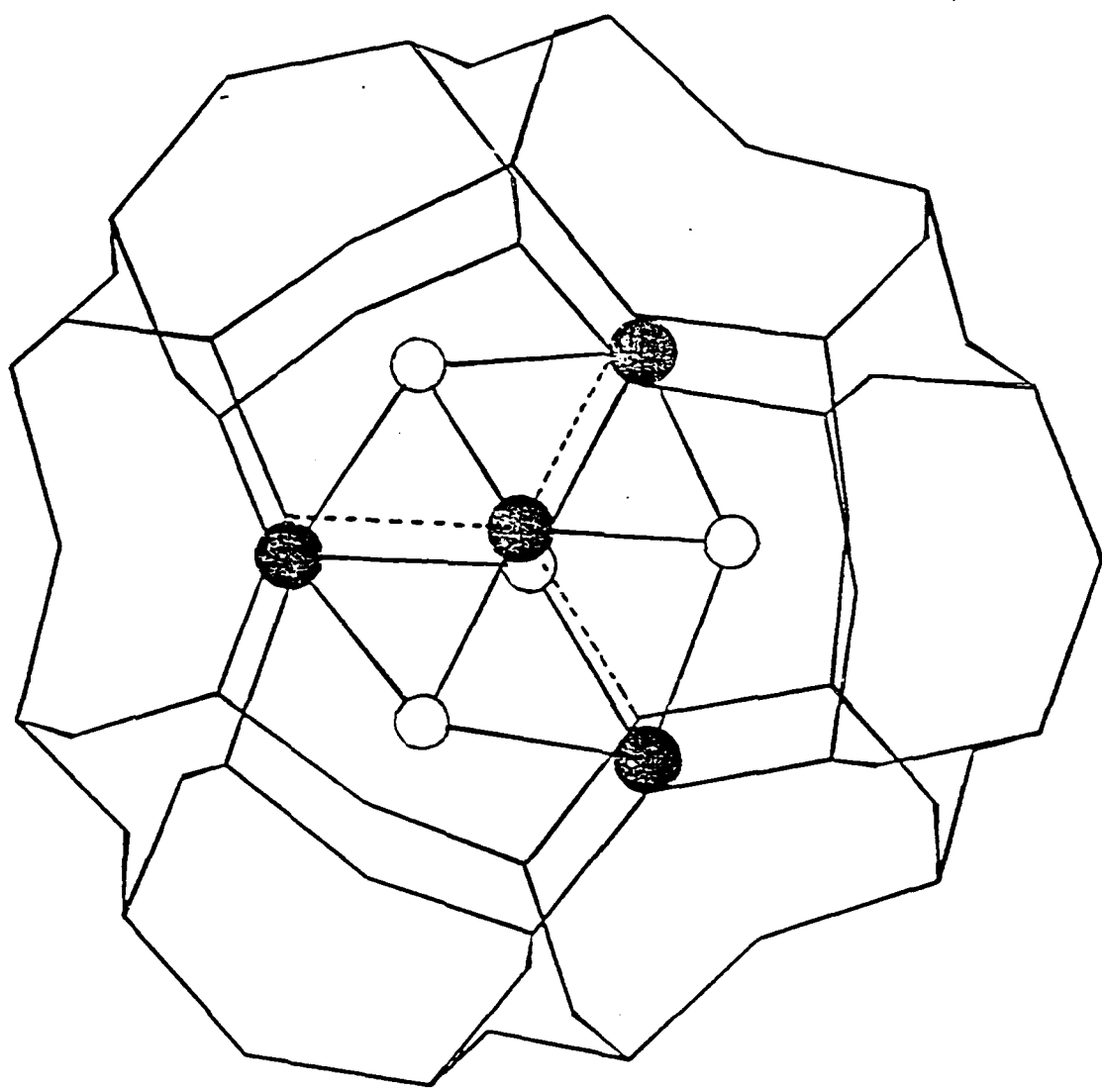
CHEM-X OCTOBER 1986

LUSTER
Fig 9-11

MAG AND IMAG PART OF TRANSF

RADIAL COORDINATE (ANGSTROM)

Fig 9

CHI ( K ** 3 )

ELECTRON WAVEVECTOR (ANGSTROM **-1)

A

MAG AND IMAG PART OF TRANSF

RADIAL COORDINATE (ANGSTROM)

B

Fig. 11